Integration of Satellite-Derived Geophysical Information into the Monitoring Framework of Monumental Buildings

International Journal of Architectural Heritage

Conservation, Analysis, and Restoration

ISSN: 1558-3058 (Print) 1558-3066 (Online) Journal homepage: www.tandfonline.com/journals/uarc20

Integration of Satellite-Derived Geophysical Information into the Monitoring Framework of Monumental Buildings

Cristian Capodicasa , Stefania Coccimiglio , Gaetano Miraglia & Rosario Ceravolo

To cite this article: Cristian Capodicasa , Stefania Coccimiglio , Gaetano Miraglia & Rosario Ceravolo (13 Aug 2026): Integration of Satellite-Derived Geophysical Information into the Monitoring Framework of Monumental Buildings, International Journal of Architectural Heritage, DOI: 10.1080/15583058.2026.2711337

To link to this article: https://doi.org/10.1080/15583058.2026.2711337

Published online: 13 Aug 2026.

INTERNATIONAL JOURNAL OF ARCHITECTURAL HERITAGE
https://doi.org/10.1080/15583058.2026.2711337

Taylor & Francis by informa

RESEARCH ARTICLE

Integration of Satellite-Derived Geophysical Information into the Monitoring Framework of Monumental Buildings

Cristian Capodicasa [a], Stefania Coccimiglio [a], Gaetano Miraglia [a,b], and Rosario Ceravolo [a,b]

[a]Department of Structural, Geotechnical and Building Engineering, Politecnico di Torino, Turin, Italy; [b]Responsible, Risk, Resilience Interdepartmental Centre (R3C), Politecnico di Torino, Turin, Italy

ABSTRACT
Understanding the influence of environmental and soil-related factors on structural response is a key challenge in long-term structural health monitoring (SHM) of heritage structures. Among these factors, soil moisture can play a significant role in soil-structure interactions (SSIs), although on-site measurements are often unavailable. This paper proposes a framework that integrates heterogeneous satellite-derived and on-site data for modelling complex, non-linear relationships between environmental variables and structural response. The methodology is based on relevance vector machines (RVMs) within the sparse Bayesian learning (SBL) paradigm and incorporates latent parameters governing the expansion order of basis functions, enabling automatic selection of informative predictors and promoting model sparsity and interpretability. Satellite-derived soil moisture products are integrated with structural, environmental, and soil measurements to reconstruct monitoring time histories and infer unobserved states influencing structural behaviour. The methodology is validated using long-term monitoring data from an extensively monitored major historic dome. Results demonstrate that satellite-derived information captures soil-related environmental effects and explains variations in structural behaviour. These findings, supported by the large-scale availability of geophysical satellite data, highlight their potential to support SHM of heritage structures, particularly where direct measurements are limited, improving the interpretation of environmental influences and enabling more efficient and informed monitoring strategies.

ARTICLE HISTORY
Received 9 April 2026
Accepted 25 July 2026

KEYWORDS
Architectural heritage; environmental and operational variations; geophysical satellite data; remote sensing; soil moisture; soil-structure interaction; structural health monitoring

1. Introduction

Modern permanent structural health monitoring (SHM) systems incorporate diverse sensor types capable of acquiring multi-physics information simultaneously, which must be cross-referenced and interpreted jointly over extended observation periods (Ceravolo et al. 2021; Gentile, Ruccolo, and Canali 2019; Lorenzoni et al. 2013). Structural variables, both static and dynamic, are known to vary in response to external influences (Ceravolo, De Marinis, et al. 2017; Rainieri and Magalhaes 2017; Roberts, Avendaño-Valencia, and García Cava 2024; Sohn 2007), commonly referred to as environmental and operational variations (EOVs). Some relevant studies addressing the influence of EOVs on the dynamic properties of monumental buildings were proposed by Ramos et al. (2010) and Saisi, Gentile, and Guidobaldi (2015). These external drivers can affect mechanical parameters and, in some circumstances, the overall structural response, introducing uncertainties into data analysis that may lead to misinterpretation of monitoring information. This issue is particularly critical in data-driven approaches, where EOV-induced changes in structural features may compromise the accuracy of the assessments. The reliable interpretation of monitoring data therefore requires distinguishing physiological variations, natural and reversible, from pathological ones, which are indicative of actual structural damage (Ceravolo, Matta, et al. 2017; Huang et al. 2018; Yang et al. 2021). In the SHM of heritage structures, this challenge is compounded by the complexity of the structural system, the variety of interacting environmental factors, and the typically long monitoring horizons involved (Gentile, Ruccolo, and Canali 2019; Kita, Cavalagli, and Ubertini 2019; Lorenzoni et al. 2013; Ubertini et al. 2017). Statistical approaches, including cointegration-based techniques, in both linear and non-linear formulations, have been proposed to disentangle EOV-induced variability from damage-related changes in dynamic features (Coletta et al. 2019). Other SHM approaches rely on the integration of heterogeneous data types and sources to provide a more comprehensive understanding of structures and their surrounding context.

CONTACT Cristian Capodicasa cristian.capodicasa@polito.it Department of Structural, Geotechnical and Building Engineering, Politecnico di Torino, Turin 10129, Italy

Given the limitations of purely on-site monitoring, particularly the cost and logistical complexity of using comprehensive sensor networks at heritage sites, growing interest has emerged in complementary data sources that can extend the spatial and temporal coverage of environmental observations. Remote sensing, and in particular satellite-based technologies, offers several practical advantages in this regard: historical archives extend back decades, spatial coverage is extensive, and no physical installation at the structure is required (Chuvieco 2020; Moreira et al. 2013). These characteristics make satellite data an attractive supplement to on-site instrumentation, especially in the early phases of a monitoring programme or when long-term retrospective analysis is needed.

In the context of SHM, the most established use of satellite data is the detection of millimetre-scale ground and structural displacements through interferometric synthetic aperture radar (InSAR). This technique has been applied to individual structures (Meng et al. 2004), infrastructures (Lazecky et al. 2015; Zhu et al. 2018), and entire urban areas (Bonano et al. 2013; Ubertini et al. 2018). More recently, attention has shifted towards other categories of satellite geophysical products that can characterise the environmental conditions surrounding a structure, including land surface temperature and soil moisture indices (Coccimiglio et al. 2022). These data can inform the modelling of EOVs and, in principle, provide information on environmental factors, such as soil conditions, that are not directly measured in conventional structural monitoring programmes. However, their use requires careful validation against *in-situ* observations, as the intrinsic characteristics of satellite sensors introduce systematic discrepancies with respect to point measurements at the structure scale (Mohanty et al. 2017).

The analysis of soil-structure interactions (SSIs) in SHM remains one of the most challenging aspects of interpreting monitoring data from civil and heritage structures (Kausel 2010; Mylonakis and Gazetas 2000; Wolf and Song 2002). The mechanical properties of soil are sensitive to environmental conditions, including moisture content and temperature, and can therefore vary seasonally in a way that influences the structural dynamic response (Boulkhiout, Messast, and Boulkhiout 2020; Brunelli, de Silva, and Cattari 2022; De Silva et al. 2019). Studies on soil-foundation-structure interaction (SFSI) and structure-soil-structure interaction (SSSI) have quantified these effects in terms of both static and dynamic response (Aldaikh et al. 2015; Banday et al. 2023; Lou et al. 2011; Luco and Contesse 1973; S. Wang and Schmid 1992), yet direct soil measurements are rarely available in operational monitoring programmes. This scarcity of soil data limits the ability to account for SSI effects in data-driven models of structural response.

Despite the growing availability of satellite geophysical products, their integration into site-specific SHM frameworks for heritage structures remains limited, or even unexplored, as in the field of monumental buildings, where implementation can be complex. In most existing studies, satellite data are used through InSAR-derived displacement time series (Tarantini et al. 2026), whereas soil-related geophysical indices, such as soil moisture products derived from radar backscatter, are rarely considered as predictors of structural response variables. As a consequence, the potential contribution of satellite soil data to long-term monitoring, particularly in terms of time-series reconstruction and the modelling of soil-related EOVs, has so far received little systematic attention. This is particularly true for monumental buildings, which rarely provide the combination of structural, environmental, and soil data needed to cross-reference satellite-derived indices against measured ground-truth.

1.1. Research significance

In full-scale SHM applications, understanding the interaction between a structure and its surrounding environment is essential for the reliable interpretation of monitoring data. Accounting for the influence of environmental and soil-related factors on structural response allows for a more informed separation of physiological variations from anomalous behaviour, ultimately enabling more efficient use of monitoring resources. Despite this recognised importance, the joint modelling of structural, environmental, and soil variables, particularly when soil data are partially or fully unavailable, remains a practical challenge in heritage structure monitoring. Due to the limited availability of long-term soil monitoring data, traditional regression models often struggle to capture such multivariate and non-linear dependencies, especially when the contributing variables are only partially observed or must be inferred from indirect sources.

To overcome these limitations, this study proposes a sparse Bayesian learning (SBL) framework as an efficient approach to model these interactions. In the SHM field, SBL has been mainly applied to damage detection problems (Chen et al. 2020; Hou et al. 2020; Q. Wang et al. 2022). By using relevance vector machines (RVMs) within the SBL framework for multi-input multi-output regression, and by incorporating latent parameters governing the selection and expansion order of the basis functions, the proposed method can capture hidden relationships between environmental and structural responses. This is especially relevant in contexts such as SSI, where confounding factors (e.g., temperature and moisture) may interact indirectly. The proposed approach provides a powerful tool capable of simplifying complex patterns and inferring unobserved states of a monitored structure, thus enabling the integration of heterogeneous data sources to reconstruct monitoring time-histories.

In the literature on data-driven SHM, various regression and machine learning approaches have been employed to characterise the relationship between structural response and environmental variables. Principal component analysis combined with regression has been widely applied to separate temperature-driven variability from potential damage-related changes in modal parameters (Deraemaeker et al. 2008). Factor models and autoregressive approaches have similarly been explored for tracking modal parameter evolution under varying environmental conditions (Reynders, Wursten, and De Roeck 2014). Gaussian process regression and related probabilistic methods offer the additional advantage of providing uncertainty quantification on predictions, which is particularly relevant in monitoring applications where the reliability of model assessments must be evaluated (Worden and Manson 2007). Cointegration-based strategies have been proposed to remove long-term environmental trends from monitoring data without explicitly modelling the underlying physical process (Coletta et al. 2019; Cross, Worden, and Chen 2011). More recently, neural network architectures and deep learning methods have been investigated for modelling complex, high-dimensional relationships between environmental inputs and structural outputs, though at the cost of reduced interpretability (Avci et al. 2021). Compared to these approaches, the SBL-RVM framework adopted here is fully probabilistic, promotes sparsity through the prior distribution over model weights, and automatically identifies the most informative combination of basis functions and predictors without requiring manual feature selection. This combination of automatic relevance determination and interpretability makes SBL-RVM particularly well-suited to the present application, where the physical role of the predictors, including satellite-derived indices, is not fully known in advance.

It should be noted that, although the SBL framework and the RVM formulation are well-established tools in machine learning and signal processing literature (Tipping 2001; Wipf and Rao 2004), their application within the SHM field, particularly for regression of environmental drivers and reconstruction of monitoring time series using satellite data, has so far received limited attention. The novelty of the present work therefore lies in the adaptation and application of these tools to the integration of heterogeneous satellite geophysical data with on-site structural and environmental monitoring records, for the purpose of time series reconstruction and improved modelling of environmental drivers in heritage building monitoring. The main objective is therefore to assess the feasibility of using satellite-derived geophysical data, in particular satellite soil moisture products, to support the reconstruction of monitoring time series and the modelling of environmental drivers of structural response, with a view to establishing a more systematic basis for the use of such data in long-term structural monitoring programmes.

The methodology is applied to the benchmark case of the Sanctuary of Vicoforte, which features a permanent dynamic and static monitoring system.

The paper is organised as follows: Section 2 presents the proposed methodology, with particular focus on the SBL modelling strategy. Section 3 describes the benchmark case and the associated monitoring data, including structural, soil-related, and environmental variables. Sections 4 and 5 present the results, while Section 6 concludes with a summary of key findings and future perspectives.

2. A sparse Bayesian learning framework for data integration

Investigating how structural response evolves under environmental and soil variations can benefit significantly from data integration. In SHM, especially when employing data-driven approaches, the type, quantity, and quality of the available data play a crucial role. The potential of data integration lies in the combination of heterogeneous data sources, which enables the extraction of complementary information and supports a more comprehensive understanding of the overall structural health condition.

Ideally, data integration requires several data types; however, this is often hindered by the limited availability of long-term monitoring systems. In this context, the approach proposed in this study integrates soil and environmental information with structural data collected from an *in-situ* monitoring system. When certain variables lack sufficiently long historical records, satellite data can play a crucial role, as they enable the reconstruction of time series and provide information for periods when data are otherwise unavailable. This study aims to investigate the influence of soil-related variables on structural response and to assess whether soil variables can be effectively estimated using remote sensing data.

To achieve these objectives, the proposed methodology introduces a flexible regression approach capable of predicting selected environmental variables within the SBL paradigm. In particular, RVMs are employed within the SBL framework and, through the use of custom basis functions, integrate multiple explanatory variables to model their relationships without requiring prior knowledge of the underlying interactions. This feature can be particularly suitable for satellite Earth observation data.

Linear correlation studies (Ezekiel 1930; Taylor 1997) can support a preliminary screening of variables worthy of further investigation. The linear correlation can be quantified using the well-known Pearson's coefficient (Benesty et al. 2009; Cohen et al. 2013; Ezekiel and Fox 1959), which takes values in the range $-1 \leq r \leq +1$: values close to $+1$ or -1 indicate strong positive and negative correlation, respectively, whereas values close to zero indicate weak linear association.

Although linear correlation studies are useful for gaining preliminary insight into the relationships between input and output quantities, such relationships are seldom purely linear. In this regard, SBL can be exploited not only to regress complex behaviours but also to assess the degree of correlation that a given output variable exhibits with respect to non-linear functions of the input variables. This is achieved by analysing the sparsity of the problem, which allows discarding basis functions whose contribution to the modelling of a specific output is negligible. This process effectively provides a form of non-linear, multidimensional correlation analysis, where varying the basis functions enables exploration of the underlying non-linear relationships.

Several goodness-of-fit indicators have been proposed in the literature to evaluate model performance (Draper and Smith 1998; Freedman 2009; Seber and Lee 2003; Tanner 2012). Among these, the normalised mean absolute error (NMAE) is adopted in the present study. NMAE is derived from the mean absolute error (MAE) and normalised by a reference value, typically the mean of the actual data. For clarity, NMAE is often expressed as a percentage.

$$NMAE = \frac{1}{n}\sum_{i=1}^{n}\frac{\left|y_i - \hat{y}_i\right|}{\bar{y}} \tag{1}$$

where n is the number of observations, y_i the measured values, $\hat{y}_i$ the predicted values, and $\bar{y}$ the mean of the observed data. Lower NMAE values indicate better regression performance.

2.1. SBL-RVM methodology with latent parameters for multi-input multi-output regression

To address multi-input, multi-output non-linear correlation and regression problems, the authors exploited an algorithm based on RVMs within the SBL framework, originally proposed by Palmer, Rao, and Wipf (2003), incorporating latent parameters for the definition of the basis functions. Regression analysis is commonly used to model the relationship between a dependent variable and one or more independent variables (Kutner et al. 2005). In this context, RVMs have been successfully embedded within the SBL paradigm (Palmer, Rao, and Wipf 2003), providing robust solutions for both regression and classification tasks (Wipf and Rao 2004). Compared to support vector machines (SVMs), RVMs typically require significantly fewer basis functions while maintaining predictive accuracy. Moreover, the Bayesian formulation of RVMs overcomes some limitations of SVMs, such as the lack of probabilistic output and reduced interpretability. A detailed comparison between SVMs and RVMs is given in Tipping (2001).

The SBL approach imposes a parameterised prior distribution over the model weights, promoting sparsity. Unlike traditional basis selection techniques, SBL-RVM does not explicitly select basis functions a priori; instead, it infers their relevance during training. A comprehensive discussion of basis selection within the SBL framework is given in Wipf and Rao (2004).

While the theoretical foundations of SBL and RVMs are well established, the contribution of this work lies in the definition of a general methodology to adapt the SBL-RVM paradigm to a SHM context characterised by heterogeneous data sources. When dealing with phenomena governed by multiple variables, the selection of the predictors is crucial in order to avoid degradation of predictive performances due to overfitting or the inclusion of weakly informative predictors. In this regard, the proposed SBL-based methodology is exploited with the aim of identifying the most informative combination of predictor variables for the problem at hand. In particular, the proposed approach supports multi-output regression and incorporates latent parameters governing the expansion order of the adopted basis functions. This formulation allows one to address practical SHM challenges, such as environmental and soil-induced variability, limited availability of long-term monitoring data, and the need for interpretable and sparse models suitable for engineering applications. As a major strength of the method, it supports the integration of satellite-derived data with on-site structural, environmental, and soil measurements.

This study builds upon the concept of a dictionary, which is widely used in the field of compressive sensing (CS) (Congrès international des mathématiciens 2006; Qaisar et al. 2013). Fuentes et al. (2019) present an application of dictionary-based representations for non-linear dynamic systems. The dictionary $\mathbf{D}$ is defined as a matrix collecting all candidate vectors assumed as basis elements for representing a signal $\mathbf{x}$:

$$\mathbf{x} = \mathbf{D}\boldsymbol{\beta} \tag{2}$$

where $\boldsymbol{\beta}$ is the vector of weights whose estimation allows reconstruction of the signal $\mathbf{x}$ through the dictionary $\mathbf{D}$.

In the proposed formulation, the dictionary is defined as $\mathbf{D} \in \mathbb{R}^{n\times p}$, where n is the number of samples for each variable, and $p = m \cdot s$ is the total number of basis functions, where m is the number of basis function types, and s is the number of input variables. Accordingly, the weights are defined as $\boldsymbol{\beta} \in \mathbb{R}^{p\times q}$, where q is the number of target (output) variables. The resulting output is $\mathbf{x} \in \mathbb{R}^{n\times q}$.

Within the CS framework, signals are subsampled through a random transformation; here, this operation is applied to both $\mathbf{x}$ and $\mathbf{D}$. Assuming sparsity of $\mathbf{x}$ in the domain of $\mathbf{D}$, the resulting regression problem can be solved using RVMs. Under the SBL paradigm, RVMs compute posterior probability distributions over both the weights and the predictions. RVMs perform standard regression by selecting a subset of relevant vectors from the dictionary $\mathbf{D}$ which adequately represent the observed data. Sparsity is enforced through the hyperparameters α, which govern the variances of the prior distribution over the weights. The observation noise is modelled for each output variable through the inverse variance parameter $\rho = \boldsymbol{\sigma}^{-2}$. Further methodological details can be found in Fuentes et al. (2019).

In the following, the regression is performed for each output variable; therefore, all the posterior quantities and hyperparameters are defined per output, although the output index is omitted for notational simplicity. As a result, the weight matrix $\boldsymbol{\beta}$ is modelled as a Gaussian distribution $\mathcal{N}(\boldsymbol{\mu}, \boldsymbol{\Sigma})$, where the covariance matrix $\boldsymbol{\Sigma} \in \mathbb{R}^{p\times p}$ and the mean vector $\boldsymbol{\mu} \in \mathbb{R}^{p}$, defined for each output variable, are given by:

$$\boldsymbol{\Sigma} = \left(\mathbf{A} + \rho\mathbf{D}^{\mathrm{T}}\mathbf{D}\right)^{-1} \tag{3}$$

$$\boldsymbol{\mu} = \rho\boldsymbol{\Sigma}\mathbf{D}^{\mathrm{T}}\mathbf{t} \tag{4}$$

where $\mathbf{t} \in \mathbb{R}^{n}$ denotes the vector of each target observation, assumed to be corrupted by noise. The matrix $\mathbf{A} \in \mathbb{R}^{p\times p}$ is diagonal and contains the hyperparameters α, defined for each output variable. These hyperparameters, together with the noise precision parameter ρ, are iteratively updated via type-II maximum likelihood (evidence maximisation) (Tipping 2001), allowing automatic pruning of irrelevant basis functions and adaptive estimation of noise precision. Their estimation requires an iterative procedure, as closed-form solutions are not available (Tipping 2001).

First, a measure of the quality of weights estimation is given by the gamma coefficients, which, in the current implementation, are defined in matrix form for each output variable as $\boldsymbol{\Gamma} \in \mathbb{R}^{p\times p}$. Its value is updated according to:

$$\boldsymbol{\Gamma} = \mathbf{I} - \mathcal{D}(\mathbf{A}\boldsymbol{\Sigma}) \tag{5}$$

where $\mathcal{D}(\cdot)$ denotes the operator that extracts the diagonal of its argument and returns a diagonal matrix. The hyperparameters are then updated as:

$$\mathbf{A} = \boldsymbol{\Gamma}\left(\mathcal{D}\left(\boldsymbol{\mu}\boldsymbol{\mu}^{\mathrm{T}}\right) + \varepsilon\mathbf{I}\right)^{-1} \tag{6}$$

where $\varepsilon > 0$ is a small regularisation constant introduced to avoid numerical instability. The inverse noise variance parameter can be instead computed as:

$$\rho = \frac{n - tr(\boldsymbol{\Gamma})}{\mathbf{r}^{\mathrm{T}}\mathbf{r} + \varepsilon} \tag{7}$$

where $\mathbf{r} \in \mathbb{R}^{n}$ denotes the residual vector between the target observations and the model predictions for each output variable:

$$\mathbf{r} = \mathbf{t} - \mathbf{D}\boldsymbol{\mu} \tag{8}$$

The above update equations are adopted from Tipping (2001) and Fuentes et al. (2019), with notation adjusted to the present formulation.

The model predictions follow a multivariate Gaussian distribution, whose predictive variance $\mathrm{V}_* \in \mathbb{R}$, defined for each time instant and output, and mean for each output $\mathbf{y}_* \in \mathbb{R}^{n}$, are defined as:

$$\mathrm{V}_* = \rho^{-1} + \mathbf{d}\boldsymbol{\Sigma}\mathbf{d}^{\mathrm{T}} \tag{9}$$

$$\mathbf{y}_* = \mathbf{D}\boldsymbol{\mu} \tag{10}$$

where $\mathbf{d}$ is the row of the dictionary matrix associated with the considered time instant. In this framework, the methodology incorporates an additional set of hyperparameters governing the prior distribution, one for each weight, and adopts a specific approximation to the full marginalisation over all weights and hyperparameters. The core of the algorithm lies in the optimisation of the sparsity-controlling hyperparameters α, and the noise precision ρ (Fuentes et al. 2019).

An important advantage of RVMs in the SBL framework is the ability to tailor the basis functions to the specific problem under investigation. In addition to the basic dictionary definition, the flexibility and relatively low computational cost of this approach make it well suited for incorporating series expansions, such as polynomial or Fourier series, directly into the dictionary. This is achieved by introducing latent parameters that govern the order of the expansion. The maximum order L of the latent parameters is fixed a priori, and the regression is iteratively performed for increasing orders from 1 to L. The optimal set of latent parameters is selected by minimising a cost function J_c that balances prediction accuracy and overfitting.

$$J_c = a \cdot E_{tr} + b \cdot |E_{val} - E_{tr}| \tag{11}$$

where E_{tr} and E_{val} represent the training and validation NMAE, respectively, and a, $b = 1 - a$ are scalar weights. A flowchart of the proposed methodology is presented in Figure 1.

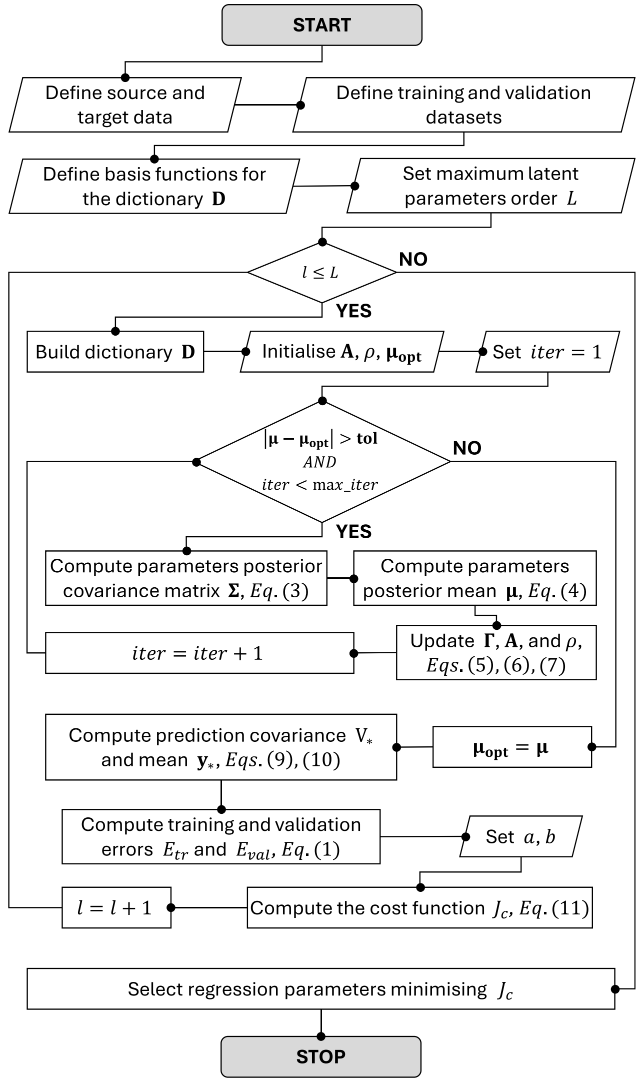

Figure 1. Flowchart of the algorithm: l denotes the loop index for latent parameter optimisation, and *iter* denotes the loop index for model weight optimisation; both indices are initialised to 1.

3. Application to the long-term monitoring data of a monumental structure

When investigating structural behaviour in relation to environmental variations, one of the major limitations in validating a model is the joint availability of different types of data. It is in fact rare to find structures equipped with extensive and diversified monitoring systems able to provide structural data together with environmental and, even more rarely, soil data. In this context, the case study becomes crucial for the objectives of the research.

The Sanctuary of Vicoforte (Figure 2) is chosen as a case study due to the extensive amount of data available from the monitoring system (Cavanni, Ceravolo, and Miraglia 2024). The structure is in fact equipped with a permanent and highly diversified monitoring system, comprising more than 120 sensors of different types, which provide continuous monitoring of its structural health. This makes the Sanctuary of Vicoforte one of the most closely monitored structures worldwide. It is one of the major works of the Piedmontese Baroque architecture; its importance is also linked to its massive oval dome. Indeed, with a major axis of 37.23 m and a minor axis of 24.89 m (Chiorino et al. 2008), it is the fifth-largest masonry dome in the world and the largest among oval masonry domes (Aoki, Chiorino, and Roccati 2003).

The Sanctuary is equipped with an extensive monitoring system. Structural monitoring began in the 1980s; in particular, in 1987 a reinforcement system was implemented using 56 post-tensioned Dywidag steel tie rods (Φ32 mm, $f_y \approx$ 1080 MPa), anchored at 14 locations around the drum (Ceravolo, De Marinis, et al. 2017). This system was designed to control the crack openings affecting the Sanctuary. Subsequently, in 2004, a low-rate monitoring system was added, which was later restored in 2024. This monitoring system includes both static and environmental sensors and consists of the following components: 56 load cells to control stresses and efficiency of the tie-bars, 12 crack meters, 2 wire gauges and 2 further laser measures, 28 thermometers installed inside and outside the Sanctuary and within the masonry, and 4 thermo-hygrometers (3 of which for measuring air relative humidity and temperature in the access place of the dome and below the sacristy, 1 for the masonry). Additionally, there is a precision barometer on the external façade of the Sanctuary at the level of the hooping system, and a pyranometer for measuring thermal flux at the lantern level on the external façade. The analyses conducted on data acquired by the static monitoring system from 2004

Figure 2. Sanctuary of Vicoforte: external (left) and internal (right) views.

to 2014 are detailed in Ceravolo, De Marinis, et al. (2017). Regarding soil monitoring, a continuous monitoring system is in place around the structure: it comprises 3 piezometers to measure groundwater depth and a thermo-hygrometer to measure soil moisture and temperature. A recent study on the geotechnical characterisation of the subsoil of the Sanctuary was carried out by Bandera, Gioffrè, and Lai (2023).

To gain a comprehensive understanding of the dynamic behaviour of the Sanctuary, a permanent dynamic monitoring system consisting of 12 mono-axial piezoelectric accelerometers was installed in December 2015 (Pecorelli et al. 2017). The dynamic monitoring data acquired in 2018, together with static and environmental measurements, are systematically analysed by Ceravolo et al. (2021) to investigate their influence on structural behaviour. This monitoring system, supported by specific algorithms, enabled the generation of long-term time series of the natural frequencies of the Sanctuary (Coccimiglio et al. 2023). Finally, the north-west bell tower is also monitored by a mixed (low and high rate) monitoring system that includes four strain-gauges to measure strain at the base, six thermometers, two laser measures, and two MEMS triaxial accelerometers.

3.1. Data processing

With over 100 sensors, the Sanctuary of Vicoforte is one of the most monitored structures in the world (Coletta et al. 2021). This exceptional level of instrumentation allows for a comprehensive and cross-referenced study of various aspects concerning both the structure itself and its surrounding context. In this work, the analysis involves structural, environmental, and soil data.

Specifically, the following data types were selected. First, *in-situ* data recorded directly from sensors that measure low-rate or slow processes, including load cells, laser distance meters, crack meters, and thermo-hygrometers, were used. These datasets were integrated with remotely acquired environmental data, such as air temperature, air relative humidity and rainfall, as well as with satellite-derived soil moisture information. For the purposes of analysis, the dataset is categorised into three groups: static, environmental, and soil-related data.

3.1.1. Static monitoring data

Regarding structural data, those from load cells (LC), laser measures (LM), and crack meters (CM) are considered. Load cells provide information about the cerclage, which reflects the stress state of the system, while the convergence distance of the dome axes offers a tangible measure of the movements of the drum-dome system. The crack meters monitor the evolution of the most significant cracking patterns of the drum system. As mentioned above, the sensors of the low-rate monitoring system have been acquiring data since 2004. A comprehensive study of the static datasets from the system startup until 2015 is given in Ceravolo, De Marinis, et al. (2017 and Ceravolo et al. 2021).

In this specific case, sensors located near the main crack of the structure, just above the dome closing ring on the west side of the building (Ceravolo, De Marinis, et al. 2017), are closely analysed. Accordingly, the following sensors have been considered: load cell LC15, located on the second of the four cerclage rings from the top (west side), laser measure LM2, which measures the major axis of the dome, and crack meter CM9, located on the main crack of the drum-dome system (Figure 3). The time series from the aforementioned sensors are shown in Figure 4. For consistency with the soil data, presented later, the analysis focuses on the overlapping period starting from November 2023.

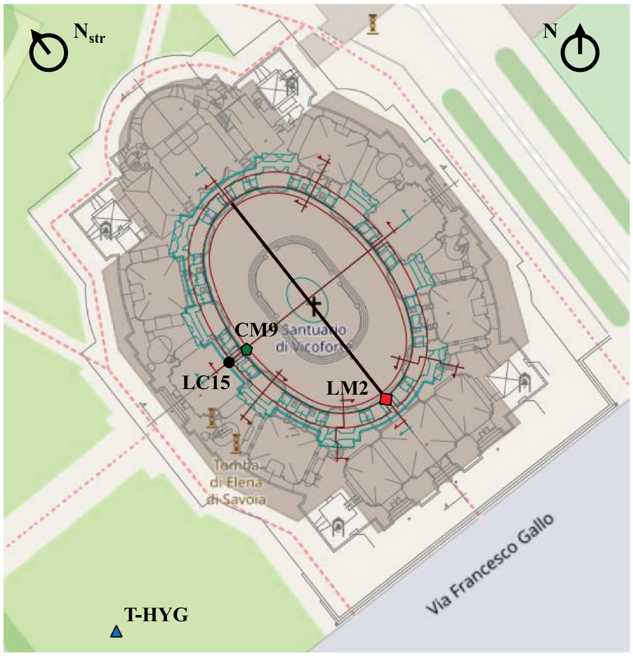

Figure 3. Layout of the Sanctuary with sensors: load cell (LC), laser measure (LM), crack meter (CM), and thermo-hygrometer (T-HYG).

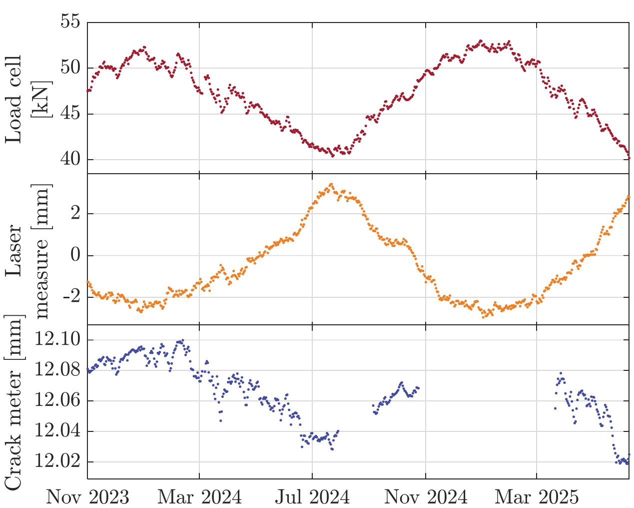

Figure 4. Selected datasets from static monitoring system: load cell (top), convergence laser measure (middle), crack meter (bottom).

These datasets result from a systematic search and removal of outliers (e.g., non-physical values), followed by daily averaging to align all data to the lowest temporal resolution. As shown in Figure 4, the datasets present clear seasonal fluctuations due to temperature variations. Notably, an increase in the major axis length corresponds to a reduction in load cell measurements and vice versa; also the minor axis shows an analogous trend. While convergence measurements are consistent with the expansion of the dome, the fluctuations observed by the load cells can be attributed to the significant difference in thermal expansion coefficients between the masonry and the steel reinforcement bars (Ceravolo et al. 2021). The cracks follow the seasonal cycle of building materials, which remains substantially stable, as long as there are no significant positive or negative trends.

3.1.2. Soil data

Among the variables that could influence soil mechanical behaviour, and consequently that of the structure (Boulkhiout, Messast, and Boulkhiout 2020), soil temperature and moisture can be identified. Both parameters can be related to satellite data. On one hand, temperature measurements do not appear to have a significant impact on soil behaviour (Coccimiglio et al. 2022), partly due to the increasing thermal inertia with depth. On the other hand, the influence of soil moisture on soil behaviour, and consequently on the SSIs, remains to be fully studied. For this reason, this work uses soil moisture data, hereinafter referred to as SM, obtained both from direct *in-situ* measurements using a thermo-hygrometer and from satellite-derived indices. The on-site sensor, called T-HYG, is located south of the building (Figure 3). It has an hourly sampling time and has the following specifications: BIT LINE, model SM-2, humidity range 0–100% Rh, humidity precision ±3% (0–50%), temperature range −40 to +80°C, temperature precision ±0.2°C, response time < 1 s.

Regarding remote sensing observation, several satellite datasets provide soil moisture information (Mohanty et al. 2017; Wagner et al. 2007). Specifically, this paper uses the soil water index (SWI) data (Raml, Bauer-Marschallinger, et al. 2025a), available through the Copernicus global land service (CGLS) with a daily time resolution. These data are derived from radar-based satellite technology, which represent an effective and reliable source. Synthetic aperture radar (SAR) sensors, in particular, are advantageous due to their independence from weather conditions and external light sources (Moreira et al. 2013). This capability makes them ideal for continuous monitoring and detecting temporal variations in specific parameters within a target area. Additionally, the SWI data, acquired by C-band radar sensors aboard the Sentinel-1 (S1) (S1 Mission, n.d.) and Meteorological Operational (MetOp) (MetOp – Earth Online, n.d.) satellites, are parameterised on reference values of a parameter called T. This parameter accounts for the depth of the so-called reservoir layer and an area-representative pseudo-diffusivity constant. The SWI soil model is described in detail in Raml, Bauer-Marschallinger, et al. (2025a, 2025b, 2025c). According to the guidelines provided by the validation report (Bauer

Marschallinger 2020), which employs the Köppen-Geiger (KG) classification (Britannica 2024), the most suitable T-values for the present case study are identified as $T = 20, 40, 60, 100$.

To ensure data reliability, the provider also delivers quality flags (QFLAGs) that serve as data confidence indicators for each SWI value. These QFLAGs range from 0% to 100%, with higher values reflecting better reliability. Specific thresholds, which vary for each T-value, distinguish whether the data is considered acceptable or not. The lower bounds adopted in this study are 55%, 60%, 65%, and 70% for T-values of 20, 40, 60, and 100, respectively, as reported in the product user manual by Raml, Bauer-Marschallinger, et al. (2025a), which tabulates the QFLAG thresholds for each T-value.

To facilitate data retrieval and processing, a dedicated application was developed in the MATLAB® environment, enabling the download of time-series data from the Copernicus land monitoring service (CLMS) (SWI full dataset, n.d.; Copernicus and ESA, n.d.) for a specified period and extraction for a designated location.

The on-site and the satellite-derived soil moisture datasets are reported in Figure 5. The on-site soil moisture is pre-processed to remove outliers and is averaged to daily samples to match the daily time resolution of the SWI satellite data. For the latter, the non-physical values and the samples with low QFLAGs are removed according to the above-defined lower bounds (Raml, Bauer-Marschallinger, et al. 2025a).

The graph of soil variables highlights how the selected SWI datasets follow the overall variation trend recorded by the on-site hygrometer, demonstrating the feasibility of using this type of satellite-derived information. Nevertheless, SWI data show a noticeable mean discrepancy and amplitude variation with respect to the on-site measurements, which may be attributed to several contributing factors. A detailed discussion of these aspects is provided in Section 4.

3.1.3. Environmental data

Given the complexity of the phenomenon, which involves both direct and indirect environmental effects, and to better understand the interacting variables, additional relevant parameters are considered based on outcomes of previous studies (Kita, Cavalagli, and Ubertini 2019; Sohn 2007; Sohn, Worden, and Farrar 2002; Ubertini et al. 2017). In particular the focus is on average air temperature, air relative humidity, and rainfall, as shown in Figure 6. All of these variables were obtained from the ARPA Piemonte website (ARPA Piemonte, n.d.) for the Mondovì (CN) station, the closest to Vicoforte (~8 km).

As expected, Figure 6 shows that air temperature follows a clear seasonal trend, unlike rainfall. It is observed that rainy periods correspond to increases in both soil moisture and SWI (Figure 5), whereas air humidity exhibits reduced variance during dry periods.

4. Correlation analysis

Data collection was followed by a pre-processing phase to remove outliers and to resample or average the datasets, thereby ensuring consistency and compatibility for subsequent analyses. An initial inspection through scatter plots was performed to identify and remove potential outliers, while also revealing possible non-linear behaviours in the data, thus underscoring the need for more advanced analyses. Subsequently, Pearson's correlation coefficients were calculated to provide a first and direct

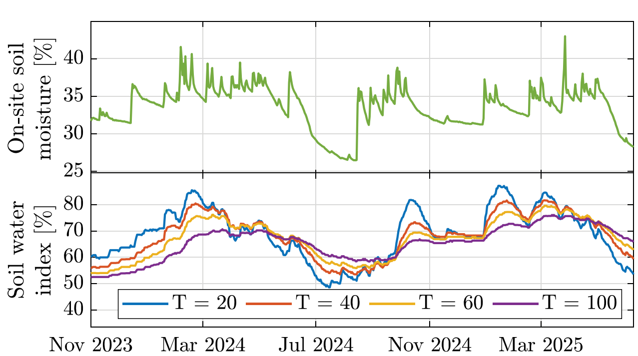

Figure 5. Soil variables: on-site soil moisture (top), satellite SWI $T = 20, 40, 60, 100$ (bottom).

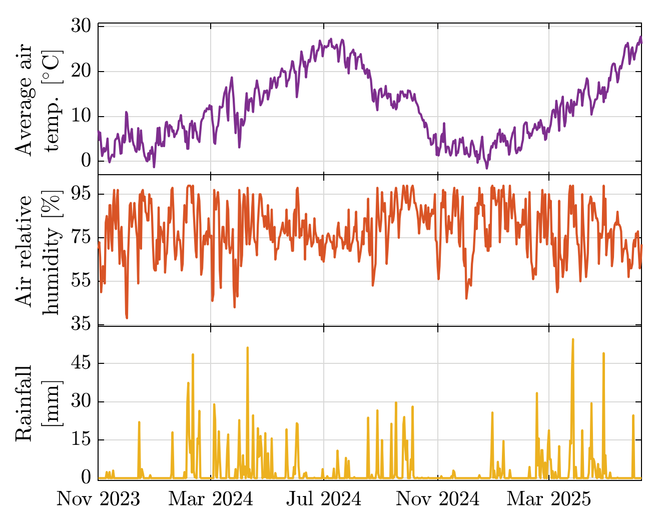

Figure 6. Environmental variables. From top to bottom: average air temperature, air relative humidity, rainfalls.

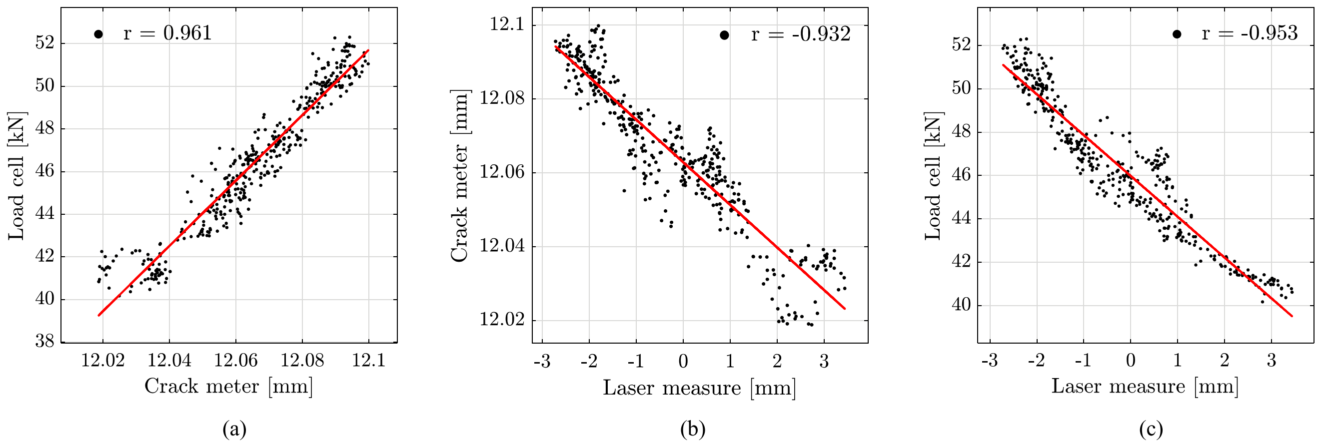

Figure 7. Correlation between: (a) LC15 and CM9, (b) CM9 and LM2, (c) LC15 and LM2.

quantification of the strength and sign of the relationships.

To develop a comprehensive understanding of the system behaviour, a correlation analysis was carried out on three structural quantities: the load cell LC15 of the hooping system, the laser measure LM2 of the dome major axis, and crack meter CM9 on the main crack. As shown in Figure 7(a), LC15 and CM9 exhibit strong positive linear correlation with a correlation coefficient $r = 0.961$, while CM9 and LM2 reveal marked negative correlation, with $r = -0.932$ (Figure 7(b)). Lastly, Figure 7(c) exhibits a strong negative linear correlation, with $r = -0.953$. All these behaviours, which are evident in the time series presented in Figure 4, confirm the seasonal pattern. Table 1 further supports this observation, showing significant linear correlations between the structural parameters and air temperature.

At this stage, before analysing the correlation between structural parameters and soil moisture, it was verified whether on-site SM data can be replaced by satellite-derived SWI within a data integration framework. To assess this feasibility, the relationship between the datasets was examined through time-series comparison, scatter plots, and correlation analysis. As shown in Table 2, the strength of the correlation varies with the T-value, with the highest value occurring at $T = 20$. For brevity, Figure 8 presents the SM-SWI

Table 1. Correlation of air temperature with structural parameters.

r	T_{air}
Load cell	−0.932
Laser measure	0.887
Crack meter	−0.924

Table 2. Correlation between SM and SWI(T).

r	SM
SWI(20)	0.622
SWI(40)	0.572
SWI(60)	0.490
SWI(100)	0.325

Figure 8. Correlation between SWI(20) and on-site SM: (a) overlapped time series and (b) scatter plot.

time-series comparison and corresponding scatterplot only for this T-value.

At first glance, the overlapped time series reveal a consistent offset between SWI(20) and SM, a pattern that is also evident for all the T-values (see Figure 5). Increasing T-values tend to reduce high-frequency noise and smooth the SWI curves, making them less sensitive to short-term SM fluctuations, particularly for $T = 60$ and $T = 100$. Conversely, SWI(20) captures rapid increases in soil moisture reasonably well, albeit with a lag or attenuation during drying phases. This delay is likely caused by the intrinsic filtering law of the SWI algorithm, which does not fully represent the actual on-site filtration, percolation and drying processes.

Despite the discrepancies arising from their different nature, the two datasets exhibit a moderate degree of correlation, as confirmed by Figure 8(b), although clear non-linearities are present. This discrepancy cannot be fully explained by a simple linear model and likely originates from fundamental differences in the physical nature, spatial scale, and temporal resolution of the two measurements. Satellite data are affected by factors such as onboard sensor types, sensor acquisition, and other aspects (Chuvieco 2020; Cracknell 2007). In particular, SWI results from significant post-processing procedures (Raml, Bauer-Marschallinger, and Sanjeevamurthy 2025b). A significant contribution to the discrepancy also stems from the difference in sensor typology: the on-site thermo-hygrometer directly measures relative humidity at a specific point, whereas the satellite-based SAR sensor indirectly estimates quantities averaged over an area with metric-scale spatial resolution. Consequently, SWI represents an interpolated, area-based, indirect value rather than a direct physical measurement. Furthermore, the physical interpretation of the parameter T remains somewhat ambiguous. Although referred to as a pseudo-physical parameter, its connection to real soil properties, such as depth, filtration behaviour, and variability among soil types, is not considered. Other variables, including temperature, ambient humidity, and natural phenomena, like evapotranspiration, are also not considered in the SWI model, further contributing to the observed differences.

Once the SWI(T) was selected to best approximate the *in-situ* soil moisture data, the correlations with the structural data were studied. In particular, the study investigates the statistical correlation between the structural monitoring data and both on-site soil moisture and SWI. The SWI(20), which showed the highest correlation with the on-site data, was taken as reference. As shown in Table 3, the correlation coefficients between structural data and on-site SM range between 0.35 and 0.55 in absolute value. However, the scatter plots in

Table 3. Correlation of structural parameters with on-site and satellite-derived soil moisture variables.

r	SM	SWI(20)
Load cell	0.350	0.668
Laser measure	−0.424	−0.709
Crack meter	0.564	0.593

Figure 9(a–c) reveal marked non-linear behaviour. Specifically, these plots suggest the presence of two distinct regimes depending on soil moisture levels. Below approximately 31% soil moisture, the relationship appears linear or slightly non-linear, whereas beyond this threshold a clear non-linearity emerges, suggesting the onset of more complex phenomena. This behaviour is less pronounced for the crack meter, which is in general more dispersed. Such dual-regime behaviour is still present, although less pronounced, in the relationship between the structural quantities and the satellite-derived index, as shown in Figure 9(d–f).

Interestingly, the correlation between SWI(20) and the three structural parameters is stronger than that observed with the on-site SM data. As shown in Table 3, correlation coefficients for SWI(20) are approximately 0.30 higher, except for the CM9, which remains substantially stable. One possible explanation is the indirect effect of temperature, given its strong correlation with the structural response. To explore this hypothesis, additional correlation analyses were performed between air temperature and both SM and SWI. The results (Table 4) show a stronger correlation between temperature and SWI than between temperature and SM, suggesting that the apparent increase in correlation between SWI and the structural parameters may be partially driven by temperature effects. In other words, temperature may amplify the apparent relationship between SWI and structural quantities.

This finding raises a question: why does air temperature correlate more strongly with SWI than with on-site SM? This could be linked to the indirect sensitivity of radar backscatter to surface temperature and evapotranspiration effects, which may influence the estimation of SWI (Raml, Bauer-Marschallinger, and Sanjeevamurthy 2025b). Further investigations are required to better understand the joint interactions among soil moisture, air temperature, and structural quantities.

Given the complexity of these interactions and the limitations and uncertainties associated with satellite-derived indices, correlation analyses cannot be relied upon alone for interpretation. The relationships observed are predominantly non-linear, and linear correlation can only provide a partial view. Therefore, a more comprehensive statistical framework is needed, one that can account for

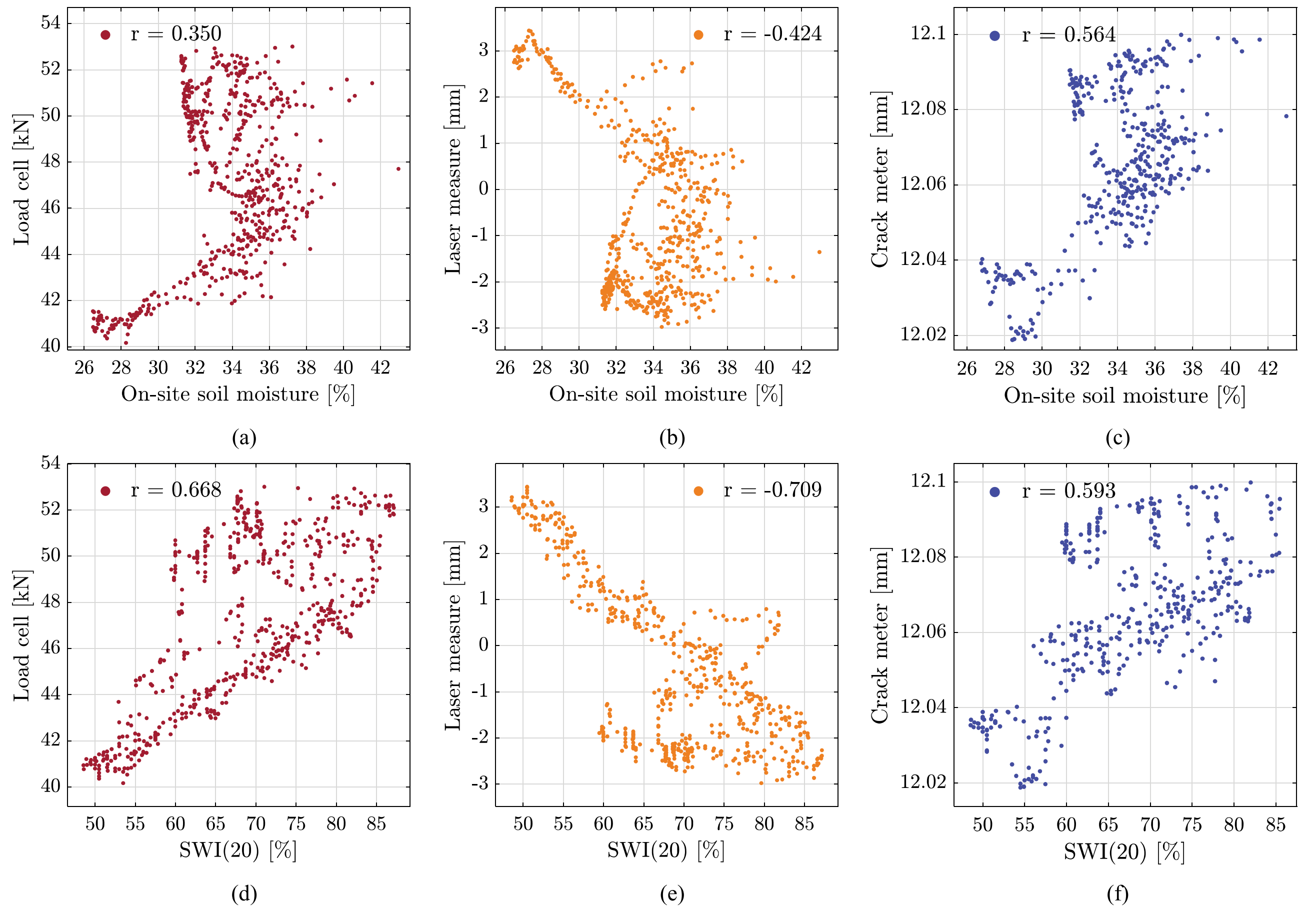

Figure 9. Correlation between: (a) LC15 and on-site SM, (b) LM2 and on-site SM, (c) CM9 and on-site SM, (d) LC15 and SWI(20), (e) LM2 and SWI(20), (f) CM9 and SWI(20).

Table 4. Correlation between air temperature and both on-site SM and SWI(20).

r	T_{air}
SM	−0.284
SWI(20)	−0.533

multiple interacting variables and capture complex, potentially non-linear relationships between on-site and satellite data. Such a framework would support a more robust assessment of whether satellite-derived information can reliably estimate soil conditions for SSI applications.

5. Satellite-informed SBL regression for reconstruction of time series

5.1. Derivation of soil moisture time series

In light of the previous considerations, the application of the regression model aims to comprehensively capture the various factors influencing soil moisture trends. Furthermore, it can be used backward to derive time series for periods prior to the installation of *in-situ* monitoring. The SBL model requires a careful definition of the basis functions, including the order of the series expansions implemented, in this case, polynomial and Fourier series. In any case, the choice of predictors strongly influences the outcomes and must be carefully assessed.

The model is trained and validated over the period from 22/09/2023 to 30/06/2025, during which the target data, i.e., the on-site soil moisture, is available. Random sampling is used to assign 70% of the dataset to training and the remaining 30% to validation. A fine-tuning process is used to identify the optimal set of basis functions in the dictionary, as well as the maximum order of latent parameters for the series expansions. In light of this, the basis functions used for soil moisture regression include the exponential and signum functions, together with series expansions based on polynomial and harmonic (Fourier-type) components. Specifically, the polynomial basis functions of order j for a predictor variable u take the form $\phi_j^P(u) = u^j$, for $j = 1, \dots, L_P$, while the harmonic components are defined as $\phi_k^S(u) = \sin(ku)$ and $\phi_k^C(u) = \cos(ku)$, for $k = 1, \dots, L_F$, where u

denotes the input variable and k is the harmonic order index. The upper bounds of these expansions, $L_F = 10$ for the harmonic order component and $L_P = 2$ for the polynomial component, were determined by manual fine-tuning. The cost function optimisation described in Section 2.1 then selects, among all combinations of active expansion orders from 1 to these upper bounds, the one that best balances training accuracy and generalisation.

Based on the outcomes of the correlation studies, the model is initially trained using SWI(20) as the sole predictor, since it shows the strongest correlation with the on-site soil moisture. Subsequently, to fully exploit the potential of the algorithm and compare different predictive configurations, additional predictors are incrementally introduced. For each configuration, the algorithm automatically selects the optimal latent parameters for the series expansions integrated into the dictionary. For this selection, the cost function defined in Eq. (11) is used, assigning a weight of 40% to the training error and 60% to the overfitting term (i.e., the difference between validation and training errors).

The comparison of goodness-of-fit metrics is reported in Table 5. These results demonstrate a significant improvement in regression quality. A first enhancement appears when all SWI time series (for the T-values suggested by the validation report; Bauer-Marschallinger 2020) are included. Further improvements are achieved by adding environmental variables considered relevant for soil moisture behaviour, namely air relative humidity (RH_{air}), rainfall (R), and air temperature (T_{air}). The improvement is substantial: the final model achieves highly accurate results, predicting the on-site soil moisture with an NMAE of approximately 2–3%.

Table 5 also indicates that, as the training and validation errors decrease, the degree of overfitting slightly tends to increase. Overall, the results show an overfitting ratio, defined as the ratio between validation and training errors, close to unity. In particular, the model trained only with SWI(20) exhibits slight underfitting, as the training error is greater than validation error, and both are relatively high. The model trained with SWI (20–100) exhibits an almost perfect balance between training and validation performance, demonstrating excellent generalisation. When additional predictors are included, particularly RH_{air} and rainfall R, a slight increase in overfitting is observed, reaching 1.16 in the fourth model configuration. This moderate tendency toward overfitting is likely related to the increased model complexity and possible multicollinearity among environmental variables. Nevertheless, the overfitting ratios remain below 1.20, confirming the good generalisation capability of the model. The last configuration exhibits almost the same errors as the fourth.

The high quality of the regression is clear in Figure 10(a), which shows the training and validation prediction datasets for the model using all predictors. The prediction (red curve) closely follows both the short-term fluctuations and the general trend of the target variable (black curve), confirming the high regression accuracy of the model. Figure 11 illustrates the optimisation of the latent parameters based on the previously defined cost function. This provides a general overview of the influence of the chosen series expansions against training and validation error, enabling a more conscious choice of maximum order and type of functions. In particular, the training and validation errors related to the soil moisture prediction with all predictors are shown per each combination of latent parameters. Each combination indicates the couple of expansion orders used in the analysis. According to the chosen maximum orders (tenth for Fourier and second for polynomial series), the first 10 combinations refer to the cases with first-order polynomials and increasing Fourier order from 1 to 10. Analogously, the second 10 (from 11 to 20) refer to the second polynomial order, again with Fourier orders from 1 to 10. The training error tends to decrease monotonically as both expansion orders increase, while the validation error shows more variable behaviour with increasing Fourier order, though it drops as a step when moving to the higher polynomial order. For each combination, the cost function is computed according to Eq. (11). As can be seen, the minimum value of the cost function is reached at the eleventh combination, which refers to the case with first-order Fourier expansion and second-order polynomial, yielding training and validation errors both below 3% and a small discrepancy between the two.

Table 5. Goodness-of-fit metrics of regression model for different predictors.

Predictors of SM	NMAE [%]		
	Training	Validation	Overfitting ratio
SWI(20)	4.592	4.548	0.990
SWI(20–100)	3.076	3.253	1.058
SWI(20–100), RH_{air}	2.776	3.063	1.103
SWI(20–100), RH_{air}, R	2.510	2.912	1.160
SWI(20–100), RH_{air}, R, T_{air}	2.598	2.951	1.139

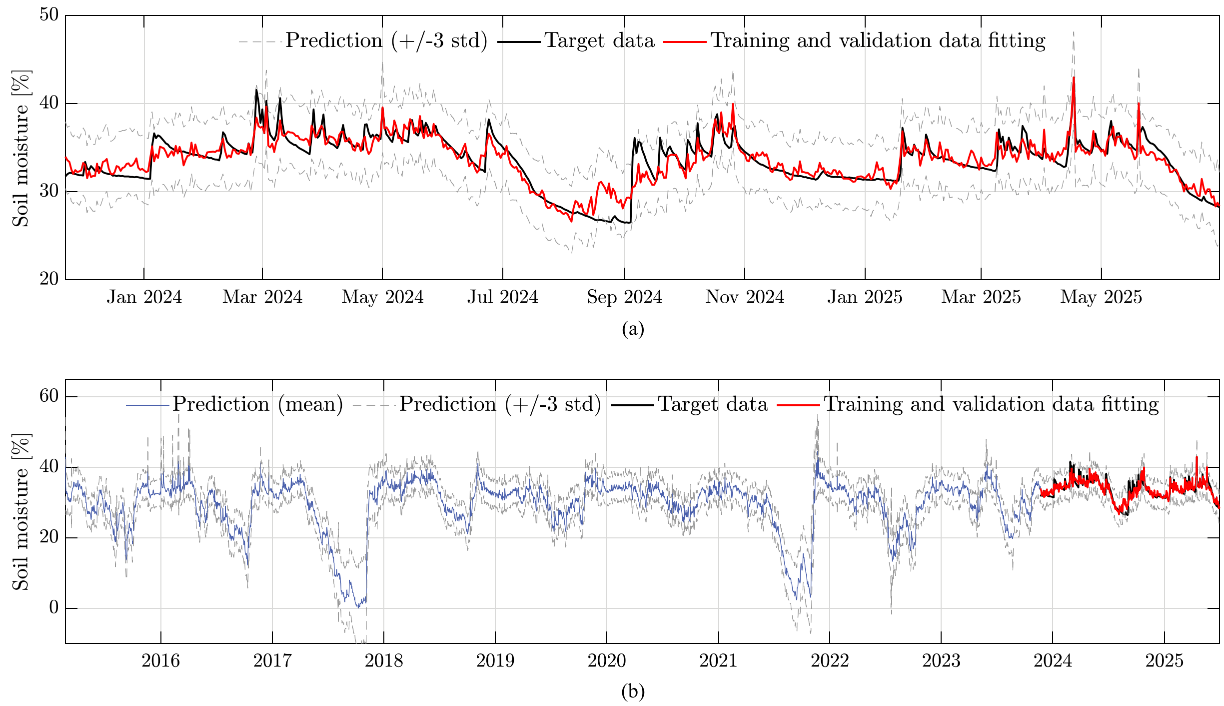

Figure 10. Soil moisture regression model: (a) training and validation datasets, (b) testing dataset.

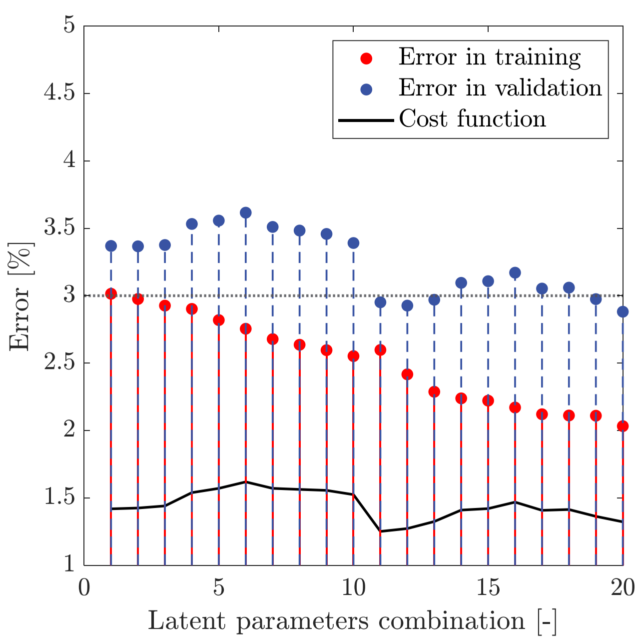

Figure 11. Training and validation errors of soil moisture prediction for each combination of latent parameters with related cost function J_c.

Once validated, the model is used to predict a new testing period starting on 23/02/2015. The results, shown in Figure 10(b), are physically consistent and align with known drought events in the Piedmont region during 2017 and 2022.

To further assess the quality of the regression, Figure 12 compares scatter plots between the structural parameters and both the predicted soil moisture and the measured target values. Given the strong dependence of the structural quantities on air temperature, this variable is also included to provide a more comprehensive view of the statistical relationships. The 3D scatter plots show that the predicted data exhibit a dispersion pattern very similar to that of the source data, further confirming the model validity. Notably, the two distinct regimes associated with soil moisture levels, previously observed in Figure 9, where the structural responses change around the 31% SM threshold, remain visible in the predicted data. The quality of the regression is further confirmed by the correlation coefficients presented in Table 6, where the normalised absolute difference remains below 10%, demonstrating the effectiveness of the proposed model.

5.2. Data-driven estimation of natural frequencies

In the field of SHM, damage detection is commonly based on the analysis of the temporal evolution of structural natural frequencies (Bassoli et al. 2017; Bicanic and Chen 1997; Farrar, Doebling, and Nix 2001; Fraraccio, Brügger, and Betti 2008). These procedures are often hindered by the presence of direct and indirect EOVs, which complicate the distinction between actual damage and physiological fluctuations (Kita, Cavalagli, and Ubertini 2019; Sohn 2007; Sohn, Worden, and Farrar 2002; Ubertini et al. 2017). In this

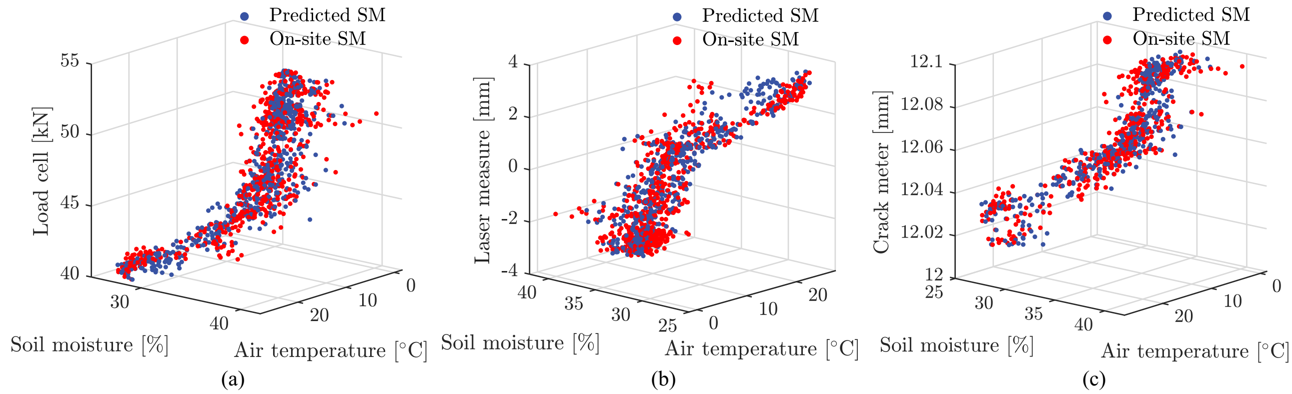

Figure 12. 3D scatterplot of environmental variables with: (a) load cell LC15, (b) laser measure LM2, (c) crack meter CM9.

Table 6. Correlation coefficient comparison of structural parameters with on-site and predicted soil moisture.

r	Source SM	Pred. SM	Normalised abs. diff. [%]
Load cell	0.3503	0.3738	6.287
Laser measure	−0.4243	−0.4767	10.997
Crack meter	0.5642	0.5795	2.640

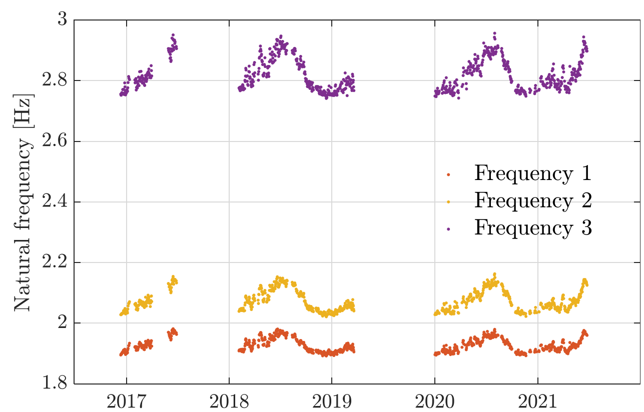

Figure 13. Time histories of the first three natural frequencies of the Sanctuary of Vicoforte.

context, the proposed framework provides a data-driven solution to model non-linear relationships associated with ambient and soil-related variables. This approach also enables the reconstruction of dynamic parameters related to unobserved structural states, while addressing the limited availability of monitoring data and the need for time-consuming identification procedures.

To complete the predictive framework, the proposed SBL-RVM regression model is employed to estimate the first three natural frequencies of the Sanctuary of Vicoforte, and then compare them with those possibly available, extracted directly from the accelerometer signals measured by the dynamic monitoring system. Modal parameter time series, in particular, were identified using the stochastic subspace identification algorithm (Pecorelli, Ceravolo, and Epicoco 2020).

The frequency time histories span the period from the beginning of 2017 to mid-2021, with some gaps in the second half of 2017 and in 2019. These gaps are mainly due to past malfunctions of the dynamic monitoring system or missing identifications, as it is not uncommon for some modes to be not identified under operational conditions (Ceravolo et al. 2021; Coccimiglio et al. 2025). The time histories of the first three natural frequencies are shown in Figure 13.

As shown in Figure 13, similarly to other structural parameters (Figure 4), all these frequencies exhibit a clear seasonal trend, increasing during warmer months and decreasing during colder periods. Specifically, the first frequency (1.88–2.00 Hz) corresponds to the first bending mode in the y direction (dome minor axis), the second frequency (2.01–2.18 Hz) to the first bending mode in x direction (dome major axis), and the third frequency (2.73–2.97 Hz) to the first torsional mode of the main body. From a structural perspective, these trends are consistent with the behaviour observed in the low-rate monitoring variables (Figure 4). In particular, the reduction in frequency during colder months coincides with the opening of the main crack of the drum system.

With the aim of reconstructing the overall behaviour of the natural frequencies, the proposed SBL-RVM regression model was applied. The same dictionary structure described in Section 5.1 is employed, with basis functions including polynomial and harmonic components. The maximum latent parameter orders are set to tenth-order for both Fourier and polynomial contributions, and the optimal expansion orders are selected by minimising the cost function of Eq. (11) independently for each of the two regression steps.

Previous studies have shown that seasonal variations in natural frequencies are mainly driven by air temperature fluctuations (Coccimiglio et al. 2022). Accordingly, the regression procedure was structured as a two-step approach. In the first step, the natural frequencies were regressed using air temperature as the sole predictor, yielding a temperature-based frequency prediction. This step captures the dominant seasonal pattern but leaves residuals that reflect contributions from other environmental variables, including soil-related factors. In the second step, the residuals with respect to the target frequencies, defined as the difference between the experimental and temperature-predicted values, were regressed using, as sole predictor, the satellite-derived soil moisture time series reconstructed in Section 5.1 for the testing period (Figure 10(b)). The on-site SM sensor data could not be used directly for this purpose, as the sensor was not installed until late 2023 and therefore provides no coverage over the 2017–2021 frequency observation period. The rationale for this sequential decomposition is twofold: it preserves the physical interpretability of each contribution and avoids merging the dominant temperature effect with the more indirect influence of soil moisture on structural dynamics. The final frequency time histories, obtained by summing the two regressed contributions, are shown in Figure 14. The high quality of the regression is confirmed by the NMAE between the target and predicted data, which remains close to 0.5% for all the considered frequencies, as reported in Table 7.

The magnitude and quality of the soil moisture-predicted residuals are illustrated in Figure 15, which shows, for each of the three frequencies, the experimental residuals, defined as the difference between the identified frequencies and the temperature-based prediction, alongside the soil moisture-based predictions. The predicted residuals range from approximately ±0.01 Hz for the first and second frequencies to slightly higher values, around ±0.015 Hz, for the third frequency, compared to experimental residuals spanning roughly ±0.03 to ±0.07 Hz depending on the mode. The model captures the general trend and sign of the experimental residuals but underestimates their amplitude. This behaviour is consistent with the indirect and second-order nature of soil moisture effects on structural dynamics: soil moisture influences structural response through SSI mechanisms that are inherently non-linear and only partially captured by a regression model trained on indirect satellite-derived data. Furthermore, the frequency identification data cover the period 2017–2021, whereas the on-site soil moisture sensor was installed in late 2023; the SM regression therefore relies entirely on satellite-derived data over this period, without the benefit of concurrent *in-situ* SM measurements to directly support model calibration over the frequency observation period. Despite this limitation, the consistent improvement in NMAE across all three modes, shown in Table 7, confirms that the satellite-derived soil moisture carries non-redundant predictive information, even if its contribution remains modest relative to temperature for the present case study.

This analysis further confirms the capability of the conceived regression framework to reconstruct dynamic monitoring variables, thereby enhancing the interpretability and usability of monitoring data in the field of SHM.

6. Conclusions

This study presents a comprehensive and predictive framework for the integration of on-site and remotely sensed environmental variables in the context of SHM, demonstrating the practical feasibility of using satellite-derived geophysical information to infer monitoring time series. The proposed methodology focuses on the use of satellite-derived data to model soil moisture dynamics and to reconstruct monitoring time series, namely modal frequencies, through a SBL-

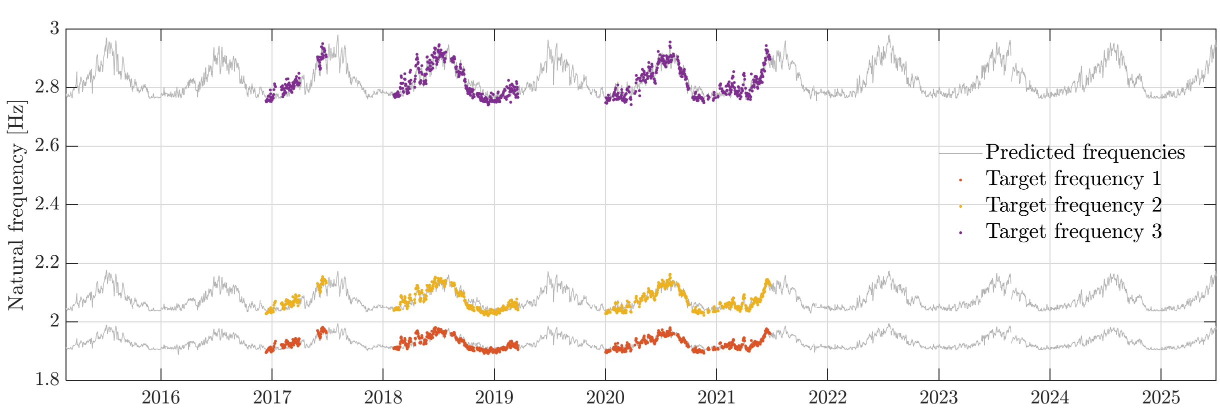

Figure 14. Regression of the first three natural frequencies of the Sanctuary of Vicoforte based on air temperature and predicted soil moisture.

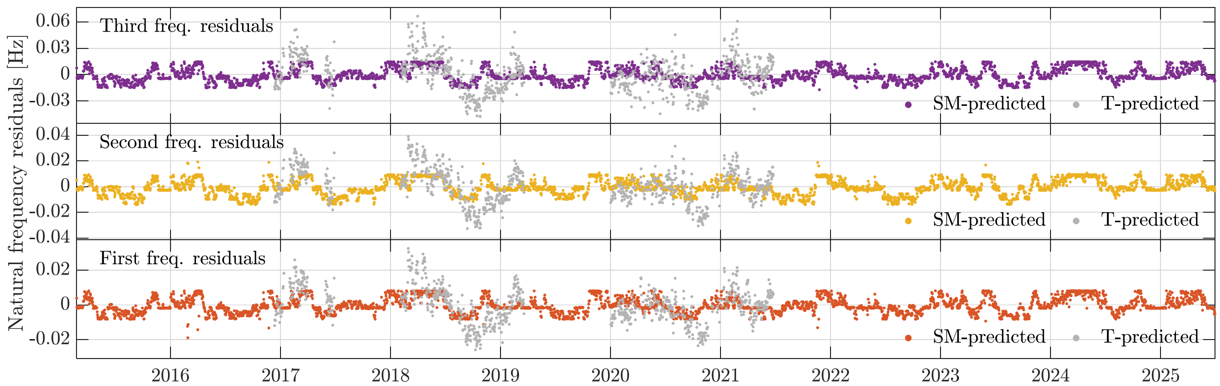

Figure 15. Residuals of the natural frequency regression after subtraction of the temperature-based contribution: T-predicted residuals (grey) and SM-predicted residuals (coloured), for the third (top), second (middle), and first (bottom) frequency.

Table 7. NMAE of the natural frequency regression model: air temperature-only prediction and combined prediction (air temperature and soil moisture).

Frequency	NMAE [%] T_{air} only	NMAE [%] T_{air} & SM	Improvement [%]
First (bending in *y* dir.)	0.428	0.388	0.040
Second (bending in *x* dir.)	0.512	0.461	0.051
Third (torsional)	0.569	0.524	0.045

RVM approach. The method is applied to the Sanctuary of Vicoforte, a monumental structure equipped with an extensive permanent monitoring system, which serves as an ideal benchmark case.

In the first part of the study, an extensive correlation analysis deepened the understanding of the relationships between structural parameters and soil-related variables. In particular, clear statistical correlations were found between structural and environmental variables, particularly soil moisture and air temperature. Moreover, the soil moisture measured through the on-site sensor and the satellite-derived index showed significant correlation with dynamic parameters, though the presence of non-linear trends (e.g., a change in structural behaviour around 31% soil moisture) limited the applicability of linear models.

Regarding the interpretation of SSI effects, the present study does not allow for a direct quantification of soil-structure interactions in terms of mechanical soil parameters. Nevertheless, the non-linear transition observed around 31% soil moisture content, visible across multiple structural parameters, suggests that moisture variations in the soil may affect the boundary conditions at the building's foundations in a non-trivial way. Whether this reflects a modification of SSI-related constraints, changes in foundation-soil contact conditions, or other moisture-mediated mechanisms remains an open question, and a more rigorous investigation would require coupling the present framework with a geotechnical model of the subsoil.

In the second part, the SBL-based regression model successfully estimated the on-site soil moisture and the natural frequencies of the structure with high accuracy, starting from remote sensing data. The best-performing configuration, integrating the satellite-derived SWI with additional environmental variables, achieved:

- normalised mean absolute error below 3% on both training and validation datasets for soil moisture regression;
- normalised absolute difference below approximately 10% when comparing predicted soil moisture with actual on-site measurements;
- statistical consistency between predicted soil moisture and structural parameters, including preservation of the previously observed dual-behaviour patterns;
- high accuracy in reconstructing natural frequencies and robust generalisation to unseen data, with realistic predictions for historical periods lacking on-site measurements or unavailable system identification results.

The developed approach demonstrates flexibility and predictive accuracy, allowing the inclusion of multiple predictors without inducing overfitting or significantly increasing computational costs. In combination with satellite data, it offers a viable alternative to costly on-site measurements and mitigates problems associated with missing or incomplete monitoring records, extending the historical coverage of key environmental parameters.

From an operational standpoint, the integration of satellite remote sensing data into SHM programmes can take several forms. First, SWI data can serve as a retrospective source of soil moisture information for periods preceding the installation of on-site sensors, enabling a longer historical baseline for statistical modelling. Second, during sensor outages or data gaps, which are not uncommon in long-term monitoring systems, satellite-derived indices can provide gap-filling data to preserve the continuity of monitoring records. Third, in the initial phases of a monitoring programme, when budget constraints may limit the number of installed sensors, satellite products can support the prioritisation of sensor placement by identifying environmental parameters that most strongly influence structural response at a given site. Finally, in the context of multi-structure or urban-scale monitoring, the spatially continuous nature of satellite data enables systematic comparisons across multiple buildings, supporting a more targeted and cost-effective allocation of monitoring resources.

Within the broader SSI context, a promising direction is the development of soil models capable of regressing mechanical soil properties from remotely sensed data, potentially combined with finite element model (FEM) techniques to link soil states with structural variables. Complementary satellite products, such as the European ground motion service (EGMS) dataset distributed through the CLMS, could offer an additional perspective through the delivery of area-wide surface displacement time series at the scale of tens of metres. The joint exploitation of ground movements and soil moisture data from satellite sources could, in principle, support the identification of ground movements associated with moisture-driven changes in SSI conditions, offering a more complete picture of the environmental drivers of structural behaviour.

Acknowledgement

This research was partially supported by the *Amministrazione del Santuario di Vicoforte and the Fondazione Cassa di Risparmio di Cuneo* and was carried out within the «SAT4SHM — Quantifying the effects of structure-soil-structure interaction on structural modal parameters by combining earth observation data with on-site dynamic monitoring: an enhanced vibration-based structural health monitoring approach» project – funded by the European Union – Next Generation EU within the PRIN 2022 program (D.D. 104 – 02/02/2022 Ministero dell'Università e della Ricerca). This manuscript reflects only the authors' views and opinions, and the Ministry cannot be considered responsible for them.

Author contributions

CRediT: **Cristian Capodicasa:** Conceptualization, Data curation, Formal analysis, Investigation, Methodology, Resources, Validation, Visualization, Writing – original draft, Writing – review & editing; **Stefania Coccimiglio:** Conceptualization, Data curation, Investigation, Methodology, Resources, Supervision, Validation, Visualization, Writing – review & editing; **Gaetano Miraglia:** Conceptualization, Data curation, Investigation, Methodology, Resources, Supervision, Validation, Visualization, Writing – review & editing; **Rosario Ceravolo:** Conceptualization, Project administration, Supervision, Writing – review & editing.

Disclosure statement

No potential conflict of interest was reported by the author(s).

Funding

The authors received no financial support for the research, authorship, and/or publication of this article.

ORCID

Cristian Capodicasa http://orcid.org/0009-0005-5633-9964
Stefania Coccimiglio http://orcid.org/0000-0002-5399-4243
Gaetano Miraglia http://orcid.org/0000-0002-3611-0215
Rosario Ceravolo http://orcid.org/0000-0001-5880-8457

Data availability statement

The datasets generated and/or analysed during the current study are available upon request.

References

Aldaikh, H., N. A. Alexander, E. Ibraim, and O. Oddbjornsson. 2015. "Two Dimensional Numerical and Experimental Models for the Study of Structure-Soil-Structure Interaction Involving Three Buildings." *Computers & Structures* 150:79–91. https://doi.org/10.1016/j.compstruc.2015.01.003.

Aoki, T., M. A. Chiorino, and R. Roccati. 2003. "Structural Characteristics of the Elliptical Masonry Dome of the Sanctuary of Vicoforte." In *Proceedings of the First*

International Congress on Construction History, edited by S. Huerta, 203–212. Madrid: Instituto Juan de Herrera.

ARPA Piemonte. n.d. Accessed November 30, 2025. http://www.arpa.piemonte.it/ .

Avci, O., O. Abdeljaber, S. Kiranyaz, M. Hussein, M. Gabbouj, and D. J. Inman. 2021. "A Review of Vibration-Based Damage Detection in Civil Structures: From Traditional Methods to Machine Learning and Deep Learning Applications." *Mechanical Systems and Signal Processing* 147:107077. https://doi.org/10.1016/j.ymssp.2020.107077.

Banday, Z. Z., X. Pu, A. Marzani, and A. Palermo. 2023. "An Analytical Approach to Model Structure-Soil-Structure Interaction (SSSI) of Arbitrarily Distributed Buildings Under SH Waves." *Engineering Structures* 292:116469. https://doi.org/10.1016/j.engstruct.2023.116469.

Bandera, S., D. Gioffrè, and C. G. Lai. 2023. "Geotechnical Characterization of the Subsoil at the 'Regina Montis Regalis' Basilica in Vicoforte, Italy." In *8th Italian Conference of Researchers in Geotechnical Engineering (CNRIG 2023)*, 5–7 July 2023, Geotechnical Engineering in the Digital and Technological Innovation Era. Springer Series in Geomechanics and Geoengineering, Palermo, Italy, edited by A. Ferrari, M. Rosone, M. Ziccarelli, and G. Gottardi, 487–494. Cham: Springer. https://doi.org/10.1007/978-3-031-34761-0_59.

Bassoli, E., M. Forghieri, L. Vincenzi, M. Bovo, and C. Mazzotti. 2017. "Structural Health Monitoring of a Historical Masonry Bell Tower Using Operational Modal Analysis." *Key Engineering Materials* 747:440–447. https://doi.org/10.4028/www.scientific.net/KEM.747.440.

Bauer-Marschallinger, B. 2020. "Copernicus Global Land Operations 'Vegetation and Energy', 'Soil Water Index, Collection 1km, Version 1.0, Issue I1.11 - Validation Report'."

Benesty, J., J. Chen, Y. Huang, and I. Cohen. 2009. "Pearson Correlation Coefficient." In *Noise Reduction in Speech Processing, Springer Topics in Signal Processing*. Berlin Heidelberg: Springer. https://doi.org/10.1007/978-3-642-00296-0_5.

Bicanic, N., and H. Chen. 1997. "Damage Identification in Framed Structures Using Natural Frequencies." *International Journal for Numerical Methods in Engineering* 40 (23): 4451–4468. https://doi.org/10.1002/(SICI)1097-0207(19971215)40:23<4451::AID-NME269>3.0.CO;2-L.

Bonano, M., M. Manunta, A. Pepe, L. Paglia, and R. Lanari. 2013. "From Previous C-Band to New X-Band SAR Systems: Assessment of the DInSAR Mapping Improvement for Deformation Time-Series Retrieval in Urban Areas." *IEEE Transactions on Geoscience & Remote Sensing* 51 (4): 1973–1984. https://doi.org/10.1109/TGRS.2012.2232933.

Boulkhiout, R., S. Messast, and R. Boulkhiout. 2020. "Effect of Soil on the Seismic Response of Structures Taking into Consideration Soil-Structure Interaction." *International Journal of Geotechnical Earthquake Engineering* 11 (2): 72–90. https://doi.org/10.4018/ijgee.2020070104.

Britannica. 2024. "Koppen Climate Classification - Definition, System, & Map." Accessed December 13, 2024. https://www.britannica.com/science/Koppen-climate-classification .

Brunelli, A., F. de Silva, and S. Cattari. 2022. "Site Effects and Soil-Foundation-Structure Interaction: Derivation of Fragility Curves and Comparison with Codes-Conforming Approaches for a Masonry School." *Soil Dynamics and Earthquake Engineering* 154:107125. https://doi.org/10.1016/j.soildyn.2021.107125.

Cavanni, V., R. Ceravolo, and G. Miraglia. 2024. "A Domain Adaptation Methodology for Enhancing the Classification of Structural Condition States in Continuously Monitored Historical Domes." *Computer-Aided Civil and Infrastructure Engineering* 39 (24): 3721–3740. https://doi.org/10.1111/mice.13313.

Ceravolo, R., G. Coletta, G. Miraglia, and F. Palma. 2021. "Statistical Correlation Between Environmental Time Series and Data from Long-Term Monitoring of Buildings." *Mechanical Systems and Signal Processing* 152:107460. https://doi.org/10.1016/j.ymssp.2020.107460.

Ceravolo, R., A. De Marinis, M. L. Pecorelli, and L. Zanotti Fragonara. 2017. "Monitoring of Masonry Historical Constructions: 10 Years of Static Monitoring of the World's Largest Oval Dome." *Structural Control & Health Monitoring* 24 (10): e1988. https://doi.org/10.1002/stc.1988.

Ceravolo, R., E. Matta, A. Quattrone, and L. Zanotti Fragonara. 2017. "Amplitude Dependence of Equivalent Modal Parameters in Monitored Buildings During Earthquake Swarms." *Earthquake Engineering and Structural Dynamics* 46 (14): 2399–2417. https://doi.org/10.1002/eqe.2910.

Chen, Z., R. Zhang, J. Zheng, and H. Sun. 2020. "Sparse Bayesian Learning for Structural Damage Identification." *Mechanical Systems and Signal Processing* 140:106689. https://doi.org/10.1016/j.ymssp.2020.106689.

Chiorino, M. A., A. Spadafora, C. Calderini, and S. Lagomarsino. 2008. "Modeling Strategies for the world's Largest Elliptical Dome at Vicoforte." *International Journal of Architectural Heritage* 2 (3): 274–303. https://doi.org/10.1080/15583050802063618.

Chuvieco, E. 2020. *Fundamentals of Satellite Remote Sensing: An Environmental Approach*. Boca Raton, FL: CRC Press.

Coccimiglio, S., G. Coletta, E. Lenticchia, G. Miraglia, and R. Ceravolo. 2022. "Combining Satellite Geophysical Data with Continuous On-Site Measurements for Monitoring the Dynamic Parameters of Civil Structures." *Scientific Reports* 12 (1): 2275. https://doi.org/10.1038/s41598-022-06284-7.

Coccimiglio, S., G. Miraglia, V. Cavanni, A. Crocetti, and R. Ceravolo. 2025. "Automated Mode Tracking via Supervised Classification and Adaptive Parameter Calibration for Seismic Monitoring with Sparse Sensors." *Bulletin of Earthquake Engineering* 23 (10): 4091–4117. https://doi.org/10.1007/s10518-025-02196-9.

Coccimiglio, S., G. Miraglia, G. Coletta, R. Epicoco, and R. Ceravolo. 2023. "Balanced Definition of Thresholds for Mode Tracking in a Long-Term Seismic Monitoring System." *Geosciences* 13 (12): 365. https://doi.org/10.3390/geosciences13120365.

Cohen, J., P. Cohen, S. G. West, and L. S. Aiken. 2013. *Applied Multiple Regression/Correlation Analysis for the Behavioral Sciences*. New York: Routledge.

Coletta, G., G. Miraglia, P. Gardner, R. Ceravolo, C. Surace, and K. Worden. 2021. "A Transfer Learning Application to FEM and Monitoring Data for Supporting the

Classification of Structural Condition States." In *European Workshop on Structural Health Monitoring, Lecture Notes in Civil Engineering*, edited by P. Rizzo and A. Milazzo, 947–957. Cham: Springer International Publishing. https://doi.org/10.1007/978-3-030-64594-6_91.

Coletta, G., G. Miraglia, M. Pecorelli, R. Ceravolo, E. Cross, C. Surace, and K. Worden. 2019. "Use of the Cointegration Strategies to Remove Environmental Effects from Data Acquired on Historical Buildings." *Engineering Structures* 183:1014–1026. https://doi.org/10.1016/j.engstruct.2018.12.044.

Congrès international des mathématiciens. 2006. *Proceedings of the International Congress of Mathematicians: Madrid, August 22–30, 2006*. Zürich: European Mathematical Society.

Copernicus and ESA. n.d. "Copernicus Land Monitoring Service." Accessed December 13, 2024. https://land.copernicus.eu/en/about.

Cracknell, A. P. 2007. *Introduction to Remote Sensing*. Boca Raton, FL: CRC Press.

Cross, E. J., K. Worden, and Q. Chen. 2011. "Cointegration: A Novel Approach for the Removal of Environmental Trends in Structural Health Monitoring Data." *Proceedings of the Royal Society A: Mathematical, Physical and Engineering Sciences* 467, 2712–2732.

Deraemaeker, A., E. Reynders, G. De Roeck, and J. Kullaa. 2008. "Vibration-Based Structural Health Monitoring Using Output-Only Measurements Under Changing Environment." *Mechanical Systems and Signal Processing* 22 (1): 34–56. https://doi.org/10.1016/j.ymssp.2007.07.004.

De Silva, F., A. Piro, A. Brunelli, S. Cattari, F. Parisi, S. Sica, and F. Silvestri. 2019. "On the Soil-structure Interaction in the Seismic Response of a Monitored Masonry School Building Struck by the 2016–2017 Central Italy Earthquake." In *Proceedings of the 7th International Conference on Computational Methods in Structural Dynamics and Earthquake Engineering (COMPDYN 2019)*, Crete, Greece, 1853–1862. https://doi.org/10.7712/120119.7041.19395.

Draper, N. R., and H. Smith. 1998. *Applied Regression Analysis*. New York: John Wiley & Sons.

Ezekiel, M. 1930. *Methods of Correlation Analysis*. New York: Wiley.

Ezekiel, M., and K. A. Fox. 1959. *Methods of Correlation and Regression Analysis: Linear and Curvilinear*. New York: John Wiley & Sons.

Farrar, C. R., S. W. Doebling, and D. A. Nix. 2001. "Vibration-Based Structural Damage Identification." Philosophical Transactions of the Royal Society of London, *Series A: Mathematical, Physical and Engineering Sciences* 359 (1778): 131–149. https://doi.org/10.1098/rsta.2000.0717.

Fraraccio, G., A. Brügger, and R. Betti. 2008. "Identification and Damage Detection in Structures Subjected to Base Excitation." *Experimental Mechanics* 48 (4): 521–528. https://doi.org/10.1007/s11340-008-9124-6.

Freedman, D. A. 2009. *Statistical Models: Theory and Practice*. New York: Cambridge University Press.

Fuentes, R., N. Dervilis, K. Worden, and E. J. Cross. 2019. "Efficient Parameter Identification and Model Selection in Nonlinear Dynamical Systems via Sparse Bayesian Learning." *Journal of Physics: Conference Series* 1264 (1): 012050. https://doi.org/10.1088/1742-6596/1264/1/012050.

Gentile, C., A. Ruccolo, and F. Canali. 2019. "Continuous Monitoring of the Milan Cathedral: Dynamic Characteristics and Vibration-Based SHM." *Journal of Civil Structural Health Monitoring* 9 (5): 671–688. https://doi.org/10.1007/s13349-019-00361-8.

Hou, R., X. Wang, Q. Xia, and Y. Xia. 2020. "Sparse Bayesian Learning for Structural Damage Detection Under Varying Temperature Conditions." *Mechanical Systems and Signal Processing* 145:106965. https://doi.org/10.1016/j.ymssp.2020.106965.

Huang, H.-B., T.-H. Yi, H.-N. Li, and H. Liu. 2018. "New Representative Temperature for Performance Alarming of Bridge Expansion Joints Through Temperature-Displacement Relationship." *Journal of Bridge Engineering* 23 (7): 04018043. https://doi.org/10.1061/(ASCE)BE.1943-5592.0001258.

Kausel, E. 2010. "Early History of Soil-Structure Interaction." *Soil Dynamics and Earthquake Engineering* 30 (9): 822–832. https://doi.org/10.1016/j.soildyn.2009.11.001.

Kita, A., N. Cavalagli, and F. Ubertini. 2019. "Temperature Effects on Static and Dynamic Behavior of Consoli Palace in Gubbio, Italy." *Mechanical Systems and Signal Processing* 120:180–202. https://doi.org/10.1016/j.ymssp.2018.10.021.

Kutner, M. H., C. J. Nachtsheim, J. Neter, and W. Li. 2005. *Applied Linear Statistical Models*. New York: McGraw-Hill.

Lazecky, M., D. Perissin, M. Bakon, J. M. de Sousa, I. Hlavacova, and N. Real. 2015. "Potential of Satellite InSAR Techniques for Monitoring of Bridge Deformations." In *2015 Joint Urban Remote Sensing Event (JURSE)*, Lausanne, Switzerland, 1–4. IEEE.

Lorenzoni, F., F. Casarin, C. Modena, M. Caldon, K. Islami, and F. Da Porto. 2013. "Structural Health Monitoring of the Roman Arena of Verona, Italy." *Journal of Civil Structural Health Monitoring* 3 (4): 227–246. https://doi.org/10.1007/s13349-013-0065-0.

Lou, M., H. Wang, X. Chen, and Y. Zhai. 2011. "Structure-Soil-Structure Interaction: Literature Review." *Soil Dynamics and Earthquake Engineering* 31 (12): 1724–1731. https://doi.org/10.1016/j.soildyn.2011.07.008.

Luco, J. E., and L. Contesse. 1973. "Dynamic Structure-Soil-Structure Interaction." *Bulletin of the Seismological Society of America* 63 (4): 1289–1303. https://doi.org/10.1785/BSSA0630041289.

Meng, X., G. Roberts, A. Dodson, E. Cosser, J. Barnes, and C. Rizos. 2004. "Impact of GPS Satellite and Pseudolite Geometry on Structural Deformation Monitoring: Analytical and Empirical Studies." *Journal of Geodesy* 77 (12): 809–822. https://doi.org/10.1007/s00190-003-0357-y.

MetOp – Earth Online. n.d. Accessed December 13, 2024. https://earth.esa.int/eogateway/missions/metop.

Mohanty, B. P., M. H. Cosh, V. Lakshmi, and C. Montzka. 2017. "Soil Moisture Remote Sensing: State-Of-The-Science." *Vadose Zone Journal* 16 (1): 1–9. https://doi.org/10.2136/vzj2016.10.0105.

Moreira, A., P. Prats-Iraola, M. Younis, G. Krieger, I. Hajnsek, and K. P. Papathanassiou. 2013. "A Tutorial on Synthetic Aperture Radar." *IEEE Geoscience and Remote Sensing Magazine* 1 (1): 6–43. https://doi.org/10.1109/MGRS.2013.2248301.

Mylonakis, G., and G. Gazetas. 2000. "SEISMIC SOIL-STRUCTURE INTERACTION: BENEFICIAL OR DETRIMENTAL?" *Journal of Earthquake Engineering* 4 (3): 277–301. https://doi.org/10.1080/13632460009350372.

Palmer, J., B. Rao, and D. Wipf. 2003. "Perspectives on Sparse Bayesian Learning." In *Advances in Neural Information Processing Systems*, edited by S. Thrun, L. Saul, and B. Schölkopf. Cambridge, MA: MIT Press.

Pecorelli, M. L., R. Ceravolo, G. De Lucia, and R. Epicoco. 2017. "A Vibration-Based Health Monitoring Program for a Large and Seismically Vulnerable Masonry Dome." In *Journal of Physics: Conference Series* 842 (1), 012009. IOP Publishing. https://doi.org/10.1088/1742-6596/842/1/012009.

Pecorelli, M. L., R. Ceravolo, and R. Epicoco. 2020. "An Automatic Modal Identification Procedure for the Permanent Dynamic Monitoring of the Sanctuary of Vicoforte." *International Journal of Architectural Heritage* 14 (4): 630–644. https://doi.org/10.1080/15583058.2018.1554725.

Qaisar, S., R. M. Bilal, W. Iqbal, M. Naureen, and S. Lee. 2013. "Compressive Sensing: From Theory to Applications, a Survey." *Journal of Communications and Networks* 15 (5): 443–456. https://doi.org/10.1109/JCN.2013.000083.

Rainieri, C., and F. Magalhaes. 2017. "Challenging Aspects in Removing the Influence of Environmental Factors on Modal Parameter Estimates." *Procedia Engineering* 199:2244–2249. https://doi.org/10.1016/j.proeng.2017.09.210.

Raml, B., B. Bauer-Marschallinger, and P. M. Sanjeevamurthy. 2025b. "Copernicus Global Land Operations Vegetation and Energy, 'CGLOPS1' - Algorithm Theoretical Basis Document - Soil Water Index Collection 1Km, Version 1 - ISSUE I1.40."

Raml, B., B. Bauer-Marschallinger, P. M. Sanjeevamurthy, C. Paulik, and T. Jacobs. 2025a. "Copernicus Global Land Operations 'Vegetation and Energy', 'CGLOPS-1' - Product User Manual - Soil Water Index Collection 1Km, Version 1 - Issue I1.50."

Raml, B., S. Massart, S. Afroozeh, and B. Bauer-Marschallinger. 2025c. "Copernicus Global Land Operations 'Vegetation and Energy', 'CGLOPS-1'-Validation Report, 'Soil Water Index, Collection 1km, Version 1.0, Issue I1.00'."

Ramos, L. F., L. Marques, P. B. Lourenço, G. De Roeck, A. Campos-Costa, and J. Roque. 2010. "Monitoring Historical Masonry Structures with Operational Modal Analysis: Two Case Studies." *Mechanical Systems and Signal Processing* 24 (5): 1291–1305. https://doi.org/10.1016/j.ymssp.2010.01.011.

Reynders, E., G. Wursten, and G. De Roeck. 2014. "Output-Only Structural Health Monitoring in Changing Environmental Conditions by Means of Nonlinear System Identification." *Structural Health Monitoring* 13 (1): 82–93. https://doi.org/10.1177/1475921713502836.

Roberts, C., L. D. Avendaño-Valencia, and D. García Cava. 2024. "Robust Mitigation of EOVs Using Multivariate Nonlinear Regression within a Vibration-Based SHM Methodology." *Mechanical Systems and Signal Processing* 208:111028. https://doi.org/10.1016/j.ymssp.2023.111028.

S1 Mission. n.d. Accessed December 13, 2024. https://sentiwiki.copernicus.eu/web/s1-mission.

Saisi, A., C. Gentile, and M. Guidobaldi. 2015. "Post-Earthquake Continuous Dynamic Monitoring of the Gabbia Tower in Mantua, Italy." *Construction and Building Materials* 81:101–112. https://doi.org/10.1016/j.conbuildmat.2015.02.010.

Seber, G. A., and A. J. Lee. 2003. *Linear Regression Analysis*. Hoboken, NJ: John Wiley & Sons.

Sohn, H. 2007. "Effects of Environmental and Operational Variability on Structural Health Monitoring." *Philosophical Transactions of the Royal Society A* 365 (1851): 539–560. https://doi.org/10.1098/rsta.2006.1935.

Sohn, H., K. Worden, and C. R. Farrar. 2002. "Statistical Damage Classification Under Changing Environmental and Operational Conditions." *Journal of Intelligent Material Systems and Structures* 13 (9): 561–574. https://doi.org/10.1106/104538902030904.

SWI full dataset. n.d. Accessed November 30, 2025. https://globalland.vito.be/download/manifest/swi_1km_v1_daily_netcdf/manifest_clms_global_swi_1km_v1_daily_netcdf_latest.txt.

Tanner, M. A. 2012. *Tools for Statistical Inference: Observed Data and Data Augmentation Methods*. New York: Springer Science & Business Media.

Tarantini, R., G. Miraglia, S. Coccimiglio, R. Ceravolo, and G. A. Ferro. 2026. "Soil Displacement Estimation from Integrated Sensing Technologies in Data-Driven Models Biased by Temporal Coherence of PS-Insar." *Land* 15 (2): 296. https://doi.org/10.3390/land15020296.

Taylor, J. 1997. *Introduction to Error Analysis, the Study of Uncertainties in Physical Measurements*. 2nd ed. Sausalito, CA: University Science Books.

Tipping, M. 2001. "Sparse Bayesian Learning and Relevance Vector Machine." *Journal of Machine Learning Research* 1:211–244. https://doi.org/10.1162/15324430152748236.

Ubertini, F., N. Cavalagli, A. Kita, and G. Comanducci. 2018. "Assessment of a Monumental Masonry Bell-Tower After 2016 Central Italy Seismic Sequence by Long-Term SHM." *Bulletin of Earthquake Engineering* 16 (2): 775–801. https://doi.org/10.1007/s10518-017-0222-7.

Ubertini, F., G. Comanducci, N. Cavalagli, A. Laura Pisello, A. Luigi Materazzi, and F. Cotana. 2017. "Environmental Effects on Natural Frequencies of the San Pietro Bell Tower in Perugia, Italy, and Their Removal for Structural Performance Assessment." *Mechanical Systems and Signal Processing* 82:307–322. https://doi.org/10.1016/j.ymssp.2016.05.025.

Wagner, W., V. Naeimi, K. Scipal, R. De Jeu, and J. Martínez-Fernández. 2007. "Soil Moisture from Operational Meteorological Satellites." *Hydrogeology Journal* 15 (1): 121–131. https://doi.org/10.1007/s10040-006-0104-6.

Wang, Q., Y. Dai, Z. Ma, Y. Ni, J. Tang, X. Xu, and Z. Wu. 2022. "Towards Probabilistic Data-Driven Damage Detection in SHM Using Sparse Bayesian Learning Scheme." *Structural Control & Health Monitoring* 29 (11). https://doi.org/10.1002/stc.3070.

Wang, S., and G. Schmid. 1992. "Dynamic Structure-Soil-Structure Interaction by FEM and BEM." *Computational Mechanics* 9 (5): 347–357. https://doi.org/10.1007/BF00370014.

Wipf, D. P., and B. D. Rao. 2004. "Sparse Bayesian Learning for Basis Selection." *IEEE Transactions on Signal Processing* 52 (8): 2153–2164. https://doi.org/10.1109/TSP.2004.831016.

Wolf, J. P., and C. Song. 2002. "Some Cornerstones of Dynamic Soil-Structure Interaction." *Engineering*

Structures 24 (1): 13–28. https://doi.org/10.1016/S0141-0296(01)00082-7.

Worden, K., and G. Manson. 2007. "The Application of Machine Learning to Structural Health Monitoring." *Philosophical Transactions of the Royal Society A* 365 (1851): 515–537. https://doi.org/10.1098/rsta.2006.1938.

Yang, X.-M., T.-H. Yi, C.-X. Qu, H.-N. Li, and H. Liu. 2021. "Performance Assessment of a High-Speed Railway Bridge Through Operational Modal Analysis." *Journal of Performance of Constructed Facilities* 35 (6): 04021091. https://doi.org/10.1061/(ASCE)CF.1943-5509.0001669.

Zhu, M., X. Wan, B. Fei, Z. Qiao, C. Ge, F. Minati, F. Vecchioli, J. Li, and M. Costantini. 2018. "Detection of Building and Infrastructure Instabilities by Automatic Spatiotemporal Analysis of Satellite SAR Interferometry Measurements." *Remote Sensing* 10 (11): 1816. https://doi.org/10.3390/rs10111816.